The Plant Cell, Vol. 17, 1360–1375, May 2005, www.plantcell.org © 2005 American Society of Plant Biologists

MicroRNA-Directed Regulation of Arabidopsis *AUXIN RESPONSE FACTOR17* Is Essential for Proper Development and Modulates Expression of Early Auxin Response Genes [W]

Allison C. Mallory,[a] David P. Bartel,[a,b,1] and Bonnie Bartel[c,1]

[a] Whitehead Institute for Biomedical Research, Cambridge, Massachusetts 02142
[b] Department of Biology, Massachusetts Institute of Technology, Cambridge, Massachusetts 02139
[c] Department of Biochemistry and Cell Biology, Rice University, Houston, Texas 77005

The phytohormone auxin plays critical roles during plant growth, many of which are mediated by the auxin response transcription factor (ARF) family. MicroRNAs (miRNAs), endogenous 21-nucleotide riboregulators, target several mRNAs implicated in auxin responses. miR160 targets *ARF10*, *ARF16*, and *ARF17*, three of the 23 *Arabidopsis thaliana ARF* genes. Here, we describe roles of miR160-directed *ARF17* posttranscriptional regulation. Plants expressing a miRNA-resistant version of *ARF17* have increased *ARF17* mRNA levels and altered accumulation of auxin-inducible *GH3*-like mRNAs, *YDK1*/*GH3.2*, *GH3.3*, *GH3.5*, and *DFL1*/*GH3.6*, which encode auxin-conjugating proteins. These expression changes correlate with dramatic developmental defects, including embryo and emerging leaf symmetry anomalies, leaf shape defects, premature inflorescence development, altered phyllotaxy along the stem, reduced petal size, abnormal stamens, sterility, and root growth defects. These defects demonstrate the importance of miR160-directed *ARF17* regulation and implicate ARF17 as a regulator of *GH3*-like early auxin response genes. Many of these defects resemble phenotypes previously observed in plants expressing viral suppressors of RNA silencing and plants with mutations in genes important for miRNA biogenesis or function, providing a molecular rationale for phenotypes previously associated with more general disruptions of miRNA function.

INTRODUCTION

MicroRNAs (miRNAs) are endogenous 21-nucleotide riboregulators that modulate gene expression in plants and animals (Bartel and Bartel, 2003; Carrington and Ambros, 2003; Bartel, 2004; Mallory and Vaucheret, 2004). In plants, miRNAs are processed from imperfectly complementary stem-loop precursor RNAs (Reinhart et al., 2002), and proper accumulation of some miRNAs depends on the nuclear activity of DICER-LIKE1 (DCL1) as well as HYL1, HEN1, and AGO1 (Park et al., 2002; Reinhart et al., 2002; Boutet et al., 2003; Kasschau et al., 2003; Han et al., 2004; Vaucheret et al., 2004; Vazquez et al., 2004a). In both plants and animals, miRNAs can direct cleavage of target mRNAs and/or inhibition of productive translation, although plant miRNAs appear to act primarily via mRNA cleavage (Lee et al., 1993; Wightman et al., 1993; Olsen and Ambros, 1999; Hutvágner and Zamore, 2002; Llave et al., 2002; Aukerman and Sakai, 2003; Kasschau et al., 2003; Tang et al., 2003; Chen, 2004; Yekta et al., 2004). Studies examining pairing requirements between miR165/166:*PHABULOSA* and miR171:*SCL6* miRNA:target pairs have revealed that mismatches in the miRNA 5′ region disrupt cleavage more effectively than mismatches in the miRNA 3′ region (Mallory et al., 2004b; Parizotto et al., 2004). Many plant and animal miRNAs do not accumulate ubiquitously, but instead are restricted to specific tissue types and developmental stages, suggesting spatial and temporal regulation of miRNA accumulation and, thus, of target expression (Carrington and Ambros, 2003; Ambros, 2004; Bartel, 2004).

Many miRNAs isolated from the dicot *Arabidopsis thaliana* are conserved in the monocot rice (*Oryza sativa*) and in other plants, implying conserved evolutionary roles for plant miRNAs (Reinhart et al., 2002; Floyd and Bowman, 2004; Jones-Rhoades and Bartel, 2004; Sunkar and Zhu, 2004; Wang et al., 2004a; Axtell and Bartel, 2005). Plant miRNAs often have extensive, evolutionarily conserved complementarity to plant mRNAs (Rhoades et al., 2002; Axtell and Bartel, 2005). This observation has enabled numerous regulatory targets to be confidently predicted (Park et al., 2002; Rhoades et al., 2002; Xie et al., 2003; Jones-Rhoades and Bartel, 2004; Sunkar and Zhu, 2004; Wang et al., 2004b), more than 50 of which have been experimentally validated in plants (Dugas and Bartel, 2004).

Plant miRNA complementary sites are usually present as single copies in the open reading frame of the target mRNA, although complementary sites in both 5′ and 3′ untranslated regions (UTRs) have been reported. This trend contrasts with the initially characterized animal miRNA complementary sites, which typically are present as multiple sites in the 3′ UTR of target mRNAs (Bartel, 2004). However, recent studies indicate that targeting of single sites and targeting within open reading frames are

[1] To whom correspondence should be addressed. E-mail bartel@rice.edu or dbartel@wi.mit.edu; fax 713-348-5154 or 617-258-6788.
The authors responsible for distribution of materials integral to the findings presented in this article in accordance with the policy described in the Instructions for Authors (www.plantcell.org) are: David P. Bartel (dbartel@wi.mit.edu) and Bonnie Bartel (bartel@rice.edu).
[W] Online version contains Web-only data.
Article, publication date, and citation information can be found at www.plantcell.org/cgi/doi/10.1105/tpc.105.031716.

widespread for mammalian miRNAs (Lewis et al., 2005; Lim et al., 2005).

Many plant miRNA targets encode transcription factors involved in cell fate determination (Rhoades et al., 2002), supporting the idea that miRNAs regulate plant development. In further support of this idea, plants impaired in miRNA accumulation, such as *dcl1*, *ago1*, *hyl1*, and *hen1* mutants (Park et al., 2002; Reinhart et al., 2002; Boutet et al., 2003; Kasschau et al., 2003; Han et al., 2004; Vaucheret et al., 2004; Vazquez et al., 2004a), and plants expressing viral suppressors of gene silencing that alter miRNA accumulation (Mallory et al., 2002; Kasschau et al., 2003; Chapman et al., 2004; Chen et al., 2004; Dunoyer et al., 2004) display dramatic anomalies during vegetative and floral development.

The overexpression of miRNAs and the expression of miRNA-resistant targets in vivo have allowed assignment of developmental roles to miR159/miR319/JAW, miR164, miR165/166, and miR172 miRNA families. These miRNAs regulate rosette leaf expansion and curvature (Palatnik et al., 2003), embryonic, vegetative, and floral organ boundary formation (Laufs et al., 2004; Mallory et al., 2004a), radial patterning (Emery et al., 2003; Juarez et al., 2004; Mallory et al., 2004b; McHale and Koning, 2004; Zhong and Ye, 2004), and floral organ identity and flowering time (Aukerman and Sakai, 2003; Chen, 2004). miR162 and miR168 likely influence development through feedback regulation of miRNA pathway components, *DCL1* and *AGO1*, respectively (Xie et al., 2003; Vaucheret et al., 2004). Particular miRNAs accumulate in response to sulfur starvation (Jones-Rhoades and Bartel, 2004), abiotic stresses (Sunkar and Zhu, 2004), or phytohormones (Achard et al., 2004; Sunkar and Zhu, 2004), suggesting that miRNAs are important not only for development but also for responses to environmental stimuli.

The phytohormone auxin influences many aspects of plant development (Rogg and Bartel, 2001; Liscum and Reed, 2002; Swarup et al., 2002; Friml, 2003; Jürgens, 2003), and the identity of several miRNA targets suggests roles for miRNAs in auxin signaling. miR160 is complementary to *AUXIN RESPONSE FACTOR10* (*ARF10*), *ARF16*, and *ARF17* (Rhoades et al., 2002), and miR167 is complementary to *ARF6* and *ARF8* (Rhoades et al., 2002; Bartel and Bartel, 2003). Thus, at least five of the 23 Arabidopsis ARF transcription factors are potentially miRNA regulated. ARFs are a plant-specific family of DNA binding proteins that control auxin-regulated transcription (Guilfoyle et al., 1998). They bind to auxin-responsive promoter elements (*AuxREs*), which are found in early auxin response genes, including *Auxin/Indole-3-Acetic Acid* (*Aux/IAA*), *SAUR*, and *GH3*, and can either enhance or repress transcription (Abel and Theologis, 1996; Ulmasov et al., 1999a, 1999b; Hagen and Guilfoyle, 2002). Most ARFs have a conserved N-terminal DNA binding domain (DBD), a nonconserved middle region conferring transcriptional repression or activation, and a conserved C-terminal dimerization domain (CTD) that can mediate ARF homodimerization and heterodimerization with Aux/IAA repressors (Guilfoyle et al., 1998; Ulmasov et al., 1999a, 1999b; Guilfoyle and Hagen, 2001; Liscum and Reed, 2002; Tiwari et al., 2003).

Aux/IAA proteins, short-lived nuclear proteins, can heterodimerize with activating ARF proteins, preventing early auxin-response gene expression (Kim et al., 1997; Rouse et al., 1998; Reed, 2001; Dharmasiri and Estelle, 2002; Kepinski and Leyser, 2002; Liscum and Reed, 2002; Tiwari et al., 2004). C-terminal domains of Aux/IAA proteins mediate heterodimerization and are conserved with the CTD of most ARF proteins. Increased auxin levels accelerate proteolysis of Aux/IAA proteins, which would allow ARF proteins to homodimerize and impose their regulatory functions on early auxin-response gene expression.

The transcriptional repressors ARF1-ARF4 and ARF9 have Pro-Ser-Thr–rich middle regions, whereas the transcriptional activators ARF5-ARF8 have Gln-Leu-Ser–rich middle regions (Ulmasov et al., 1999b; Tiwari et al., 2003). These observations suggest that ARFs can be classified as activators or repressors based on the amino acid composition of their middle regions. In addition, most tested ARFs require CTD-mediated dimerization to bind stably to *AuxREs* in vitro (Ulmasov et al., 1997, 1999a); however, ARF1 does not require the CTD to bind *AuxREs* in vitro (Ulmasov et al., 1997, 1999a), and ARF3 lacks a CTD. ARF10 and ARF16 display typical ARF sequence characteristics: each has a conserved DBD and CTD and a nonconserved middle region. By contrast, ARF17 is unusual because it lacks a conserved CTD, which is present in 21 of 23 Arabidopsis ARF proteins (Ulmasov et al., 1997, 1999a; Hagen and Guilfoyle, 2002).

miR160 and target ARFs are conserved in dicots and monocots (Rhoades et al., 2002; Bartel and Bartel, 2003), but the importance of miR160-directed regulation of *ARF17*, *ARF16*, and *ARF10* has not been explored. These three ARFs comprise a subgroup of Arabidopsis ARF proteins (Remington et al., 2004). *arf10* and *arf16* loss-of-function mutants do not display obvious developmental anomalies (Okushima et al., 2005), and *ARF17* has not been characterized in vivo. Here, we demonstrate that disrupting miR160 regulation of *ARF17* increases *ARF17* mRNA levels, leads to severe developmental abnormalities, including defects in embryonic, root, vegetative, and floral development, and alters *GH3*-like gene expression. These results indicate that miR160-directed regulation is critical for the developmental functions of ARF17 and expose ARF17 as a possible transcriptional regulator of *GH3*-like early auxin-response genes.

RESULTS

miR160 Regulates *ARF10*, *ARF16*, and *ARF17* Expression

We detected fragments of *ARF10*, *ARF16*, and *ARF17* mRNAs from Arabidopsis tissues and mapped the end of each fragment to precisely the nucleotide predicted for miR160-directed cleavage (Figure 1A) using a modified form of rapid amplification of cDNA ends (5′ RACE) (Llave et al., 2002). This analysis confirmed what had been reported for *ARF10* and *ARF17* (Kasschau et al., 2003) and indicated that *ARF16* also is posttranscriptionally regulated by miR160. To determine the tissues in which miR160 regulates *ARF10*, *ARF16*, and *ARF17* mRNAs, we assayed RNA accumulation in a variety of wild-type Arabidopsis tissues using gel blot analysis. We found miR160 and *ARF10*, *ARF16*, and *ARF17* full-length mRNAs in all tissues analyzed (Figure 1B), indicating that these genes are widely expressed. In addition to full-length transcripts, mRNAs the size of predicted *ARF10*, *ARF16*, and *ARF17* 3′ cleavage products were detected in all

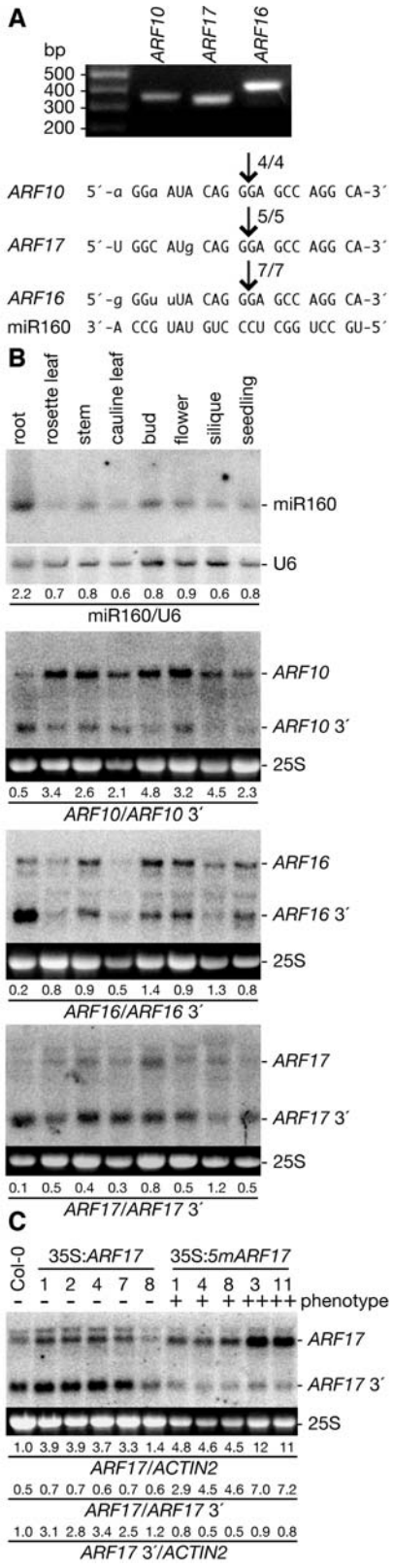

Figure 1. miR160 Regulates *ARF10*, *ARF16*, and *ARF17* in Vivo.

(A) miR160 cleavage sites in *ARF10*, *ARF16*, and *ARF17* mRNAs determined by RNA ligase-mediated 5′ RACE. The agarose gel shows the nested PCR products representing the 3′ cleavage fragments that were cloned and sequenced for each gene. The frequency of 5′ RACE clones corresponding to each cleavage site (arrows) is shown as a fraction, with the number of clones matching the target message in the numerator. As expected for miRNA-directed cleavage (Llave et al., 2002), the clones ended at the nucleotide that pairs with the 10th nucleotide of miR160. Mismatched nucleotides are in lowercase letters.

(B) miR160 and *ARF10*, *ARF16*, and *ARF17* mRNAs accumulate differentially in Arabidopsis (Col-0) tissues. Shown is an RNA gel blot analysis of 30 μg total RNA prepared from root, rosette leaf, stem, cauline leaf, buds and inflorescence meristems (bud), flower, seedpods and embryos (silique), and 12-d-old seedling tissues with a DNA probe complementary to miR160. The blot was stripped and reprobed with an oligonucleotide complementary to U6 as a loading control. Also shown is RNA gel blot analysis of 7 μg of the same RNA with RNA probes complementary to 3′ *ARF10*, 3′ *ARF16*, or 3′ *ARF17*. The positions of full-length mRNAs and 3′ cleavage products are noted at the right. Ethidium bromide staining of 25S rRNA is shown as a loading control. Ratios of miR160 to U6 RNA or *ARF* full-length mRNA to 3′ cleavage product are indicated below each lane.

(C) RNA gel blot analysis of 10 μg total RNA from rosette leaves of wild-type Col-0, *35S:ARF17*, and *35S:5mARF17* T1 plants with a 3′ *ARF17* probe. The absence (−) or presence of a moderate (+) or severe (++) rosette leaf phenotype and individual transformant numbers are indicated above the lanes. The positions of full-length *ARF17* mRNA and *ARF17* 3′ cleavage product are noted at the right. The 25S rRNA is shown as a loading control. The blot was rehybridized with an *ACTIN2* probe, and normalized values of *ARF17* full-length mRNA and *ARF17* 3′ cleavage product to *ACTIN2* (At3g18780) RNA (with Col-0 levels set at 1.0) and ratios of *ARF17* full-length mRNA to 3′ cleavage product are indicated.

tissues analyzed (Figure 1B), suggesting that miR160 is post-transcriptionally regulating these messages in many cells of the plant. The accumulation of miR160 and *ARF10*, *ARF16*, and *ARF17* 3′ cleavage products was highest in roots (Figure 1B), but there was no simple correlation among the level of miR160 and full-length *ARF* mRNA accumulation in the tissues analyzed (Figure 1B). The relative abundance of *ARF17* 3′ cleavage product compared with full-length *ARF17* mRNA in many tissues (Figure 1B) suggested extensive miRNA-directed cleavage of this transcript and prompted us to explore *ARF17* regulation in more detail.

35S:ARF17 Plants Overaccumulate *ARF17* 3′ Cleavage Product

To assess the importance of *ARF17* transcriptional regulation during development, we expressed an *ARF17* genomic clone in wild-type Arabidopsis under the control of the 35S promoter of *Cauliflower mosaic virus* (CaMV), which drives strong constitutive expression (Cary et al., 2002). Among 23 *35S:ARF17* primary transformants, 21 displayed no obvious developmental defects, whereas two displayed a slight reduction in rosette leaf size and overall stature (data not shown). RNA gel blot analysis revealed a threefold to fourfold increase in full-length *ARF17* mRNA accumulation in rosette leaves of four out of five *35S:ARF17* primary transformants, including the two smaller plants

(*35S:ARF17*-1 and *35S:ARF17*-4) (Figure 1C). The level of miR160-directed *ARF17* 3′ cleavage product also was increased approximately threefold in these four *35S:ARF17* plants compared with wild-type Columbia-0 (Col-0) (Figure 1C). The modest increase in *ARF17* mRNA expression in *35S:ARF17* Arabidopsis plants prompted us to test the efficacy of our *35S:ARF17* construct with an *Agrobacterium tumefaciens*–mediated transient expression assay in *Nicotiana benthamiana* leaves. Although we did not detect endogenous *ARF17* mRNA in *N. benthamiana* leaves, high levels of *ARF17* full-length mRNA accumulated after Agrobacterium inoculation with the *35S:ARF17* construct (data not shown), indicating that the *35S:ARF17* construct was capable of driving high level expression. The relatively low level of *ARF17* mRNA and the increased level of *ARF17* 3′ cleavage product in *35S:ARF17* Arabidopsis plants (Figure 1C), along with the wide miR160 expression profile in wild-type plants (Figure 1B), suggested that endogenous miR160 may be sufficiently abundant to direct cleavage of much of the excess *ARF17* mRNA that results from 35S driven expression, at least in the relevant tissues.

Plants Expressing miR160-Resistant *ARF17* Have Dramatic Developmental Defects

The above results suggested that posttranscriptional regulation limits *ARF17* mRNA accumulation. To examine the importance of miR160 in this regulation, we constructed a miR160-resistant version of *ARF17*. This construct, designated *5mARF17*, had five silent mutations within the miR160-complementary domain of an *ARF17* genomic clone, thereby increasing the number of mismatches between miR160 and the *ARF17* mRNA from one in wild type to six without altering the amino acid sequence of the encoded ARF17 protein (Figure 2A). These substitutions also created an *Apa*LI restriction site (Figure 2A) that allowed us to distinguish RT-PCR products of *5mARF17* transcripts from those of *ARF17*.

To determine whether miR160-directed cleavage of *5mARF17* RNA was reduced, we used an in vitro assay that relies on miRNA-programmed silencing complexes endogenously present in wheat germ extract (Tang et al., 2003), which can direct cleavage of wild-type *ARF17* RNA (G. Tang, M. Jones-Rhoades, D.P. Bartel, and P. Zamore, unpublished data), consistent with the presence of a miR160 locus in wheat (*Triticum aestivum*) (Jones-Rhoades and Bartel, 2004) and the cloning of miR160 from wheat germ extract (R. Rajagopalan and D.P. Bartel, unpublished data). For wild-type *ARF17* RNA, but not for *5mARF17* RNA, a product of the size expected for miR160-directed cleavage was detected, demonstrating that *5mARF17* mismatches interfered with miR160-directed *ARF17* cleavage (Figure 2B).

To assess the in vivo consequences of disrupting miR160 regulation, we transformed wild-type Arabidopsis plants with *5mARF17* and control *ARF17* genomic constructs under the control of the native *ARF17* 5′ and 3′ regulatory sequences. To preserve endogenous *ARF17* transcriptional regulation, we included 1.9 kb of 5′ flanking sequence, which extends ~120 bp into the annotated 3′ UTR of the upstream gene At1g77840 (~60 bp downstream of the At1g77840 stop codon), and 1.7 kb of 3′ flanking sequence, which stops 170 bp upstream of the stop codon of the downstream, reverse-oriented gene At1g77855 (Figure 2A).

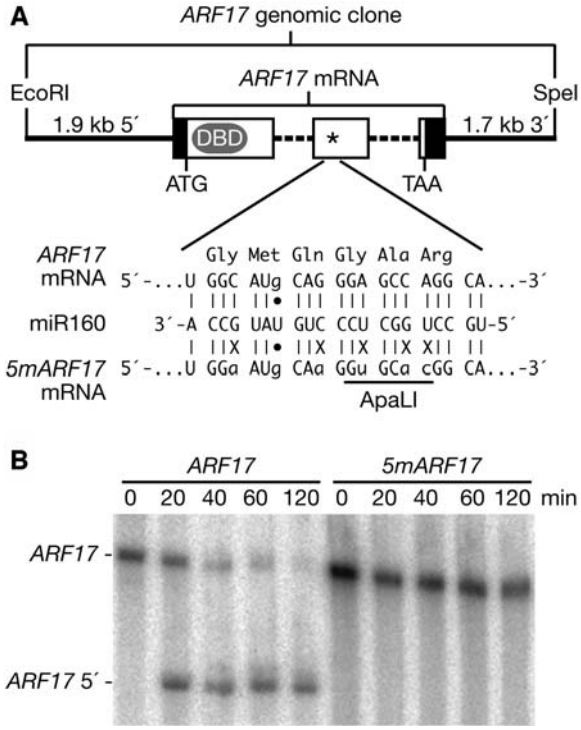

Figure 2. *5mARF17* RNA Is Resistant to miR160-Directed Cleavage.

(A) Illustration of the *ARF17* genomic clone used to transform Arabidopsis. Locations of the intergenic sequences (solid lines), introns (dashed lines), 5′ and 3′ UTRs (black boxes), DBD, remainder of the *ARF17* open reading frame (open boxes), start (ATG) and stop (TAA) codons, miR160 complementary site (asterisk), and the *Eco*RI and *Spe*I sites used for cloning are shown. mRNA segments from *ARF17* and *5mARF17* are shown paired with miR160, with the *Apa*LI restriction site unique to *5mARF17* and the protein sequence encoded by the miR160 complementary sites of both mRNAs indicated.

(B) *ARF17* RNA cleavage directed by miR160 in wheat germ extracts. The 5′-radiolabeled transcripts prepared from wild-type *ARF17* and *5mARF17* constructs were introduced into wheat germ extracts, and the time course of cleavage was examined on a denaturing polyacrylamide gel. The positions of *ARF17* RNA and 5′ *ARF17* cleavage product are noted at the left.

None of the 101 control *ARF17* primary transformants displayed obvious or consistent developmental anomalies (Figures 3 and 4). By contrast, 51 of 90 *5mARF17* transformants displayed prominent vegetative and floral defects, including rosette and cauline leaf margin serration (Figures 3E to 3I), upward curling of the leaf margins (Figures 3E to 3I), reduced plant size (Figures 3E to 3I), accelerated flowering time (Figures 3G to 3I), altered phyllotaxy along the primary and lateral stems (Figures 4I and 4J), reduced petal size (Figures 4A to 4E), abnormal stamen structure (Figures 4F to 4H), and reduced fertility (Figures 4I and 4J). Eight of the 51 *5mARF17* transformants with developmental abnormalities died before the transition to flowering, and five plants flowered successfully but were sterile.

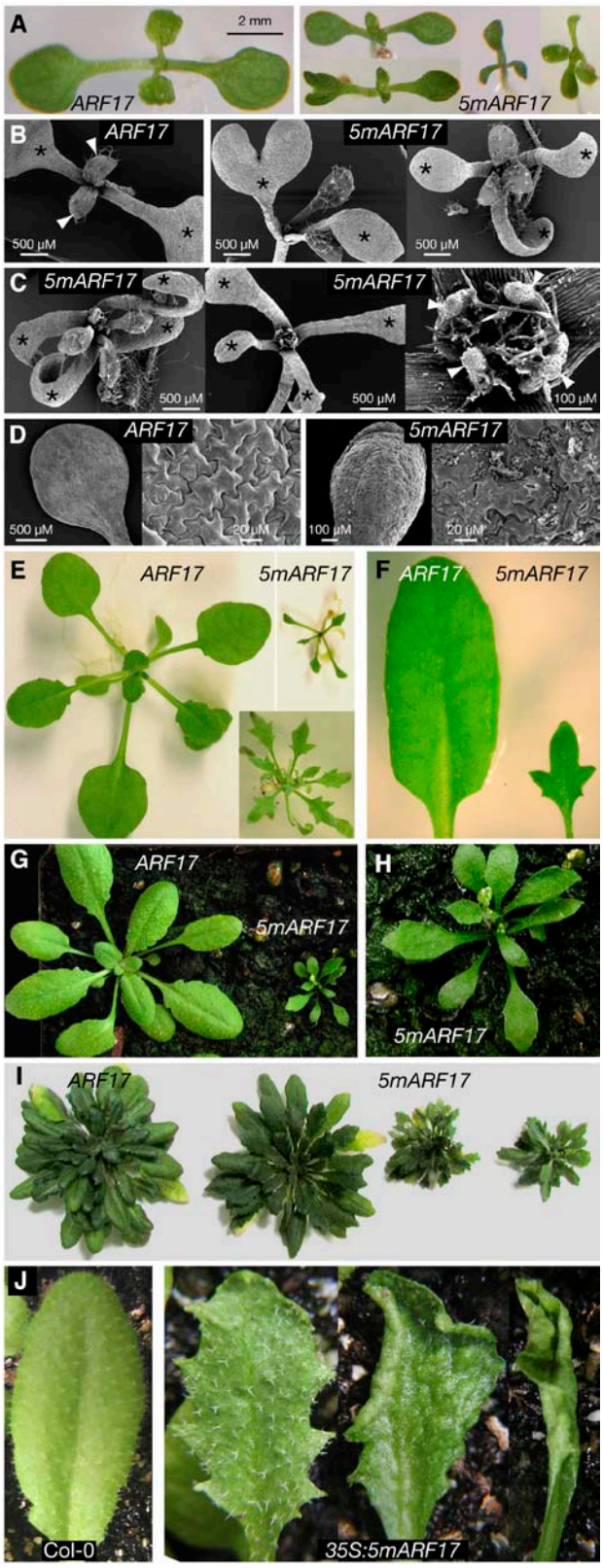

Figure 3. Embryonic and Vegetative Developmental Defects of *5mARF17* Plants.

5mARF17 progeny plants displayed presumed embryonic defects, including symmetry anomalies in which the normally bilateral symmetry of germinating seedlings was instead trilateral or quadrilateral, resulting in one or two extra cotyledons (Figures 3A to 3C). Two individual hemizygous *5mARF17* plants segregated 10% (9/89) and 14% (11/81) progeny with three cotyledons and 3% (3/89) and 4% (3/81) progeny with four cotyledons. Plants with three cotyledons had three simultaneously emerging first true leaves (Figure 3B) at a frequency of 6/9 and 7/11, whereas plants with four cotyledons always had four simultaneously emerging first true leaves (Figure 3C). In addition to cotyledon-number defects, *5mARF17* cotyledons were often moderately or deeply lobed (heart shaped) and downwardly curled (Figures 3A to 3C). Abaxial cotyledon epidermal cells were altered in shape, size, and distribution (Figure 3D), perhaps contributing to the downward curling of the cotyledons. By contrast, adaxial epidermal cells of *5mARF17* cotyledons appeared relatively normal (data not shown). *5mARF17* plants displaying mild embryonic phenotypes (moderately lobed cotyledons) had mild vegetative and floral organ defects, whereas plants displaying more severe embryonic phenotypes (heart-shaped or extra cotyledons) had more severe vegetative and floral organ defects. *5mARF17* seedlings also displayed reduced root and hypocotyl lengths and decreased root branching (Figure 4M). Like the primary transformants, *5mARF17* progeny plants flowered slightly earlier than control plants. Five independent

(A) Eight-day-old control *ARF17* and *5mARF17* T2 seedlings displaying a range of embryonic phenotypes, including lobed cotyledons (bottom left of *5mARF17* panel) and extra cotyledons indicative of trilateral and quadrilateral embryonic symmetry (right *5mARF17* panels).

(B) Scanning electron micrographs of a 6-d-old control *ARF17* (left) plant with the normal two cotyledons (asterisks) and two emerging true leaves (arrowheads) and 10-d-old *5mARF17* seedlings (middle and right). The middle plant displays a lobed cotyledon and a downwardly curled cotyledon, and the right plant has three cotyledons (asterisks) and three emerging true leaves (trilateral symmetry).

(C) Scanning electron micrographs of a 10-d-old *5mARF17* seedling (left), 6-d-old *5mARF17* seedling (middle), and magnified view of the 6-d-old *5mARF17* shoot apex (right). Indicative of quadrilaterally symmetric embryos, the *5mARF17* seedlings had four cotyledons (asterisks) and four emerging rosette leaves (arrowheads) rather than two of each.

(D) Scanning electron micrographs of abaxial surfaces of 6-d-old control *ARF17* and *5mARF17* cotyledons showing altered epidermal cell shape and organization in the *5mARF17* cotyledon.

(E) Twenty-two-day-old control *ARF17* (left) and *5mARF17* (top right) T2 plants and a 30-d-old *5mARF17* T2 plant with severe leaf serration (bottom right).

(F) Rosette leaves from 30-d-old control *ARF17* (left) and *5mARF17* (right) T2 plants.

(G) Thirty-two-day-old control *ARF17* (left) and *5mARF17* (right) T1 plants. The *5mARF17* plant has bolted.

(H) Magnified view of *5mARF17* plant in **(G)**.

(I) Seventy-two-day-old control *ARF17* and three *5mARF17* T2 plants grown in short days (8 h light, 16 h dark). The *5mARF17* developmental defects are increasing in severity from left to right; only the plant with the most severe phenotype has bolted.

(J) Col-0 and *35S:5mARF17* rosette leaves with defects increasing in severity from left to right.

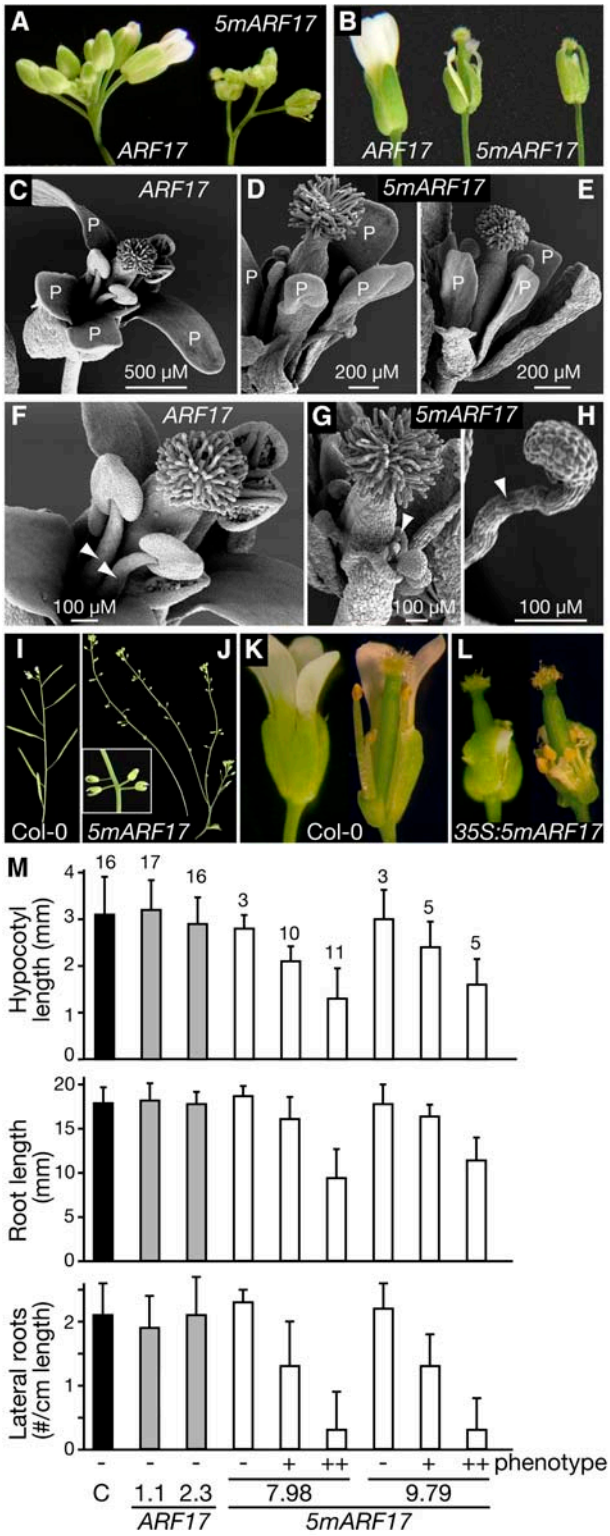

Figure 4. Floral Organ and Seedling Defects of *5mARF17* Plants.

(A) Side view of the inflorescence bud cluster of *ARF17* and *5mARF17* T1 plants.

(B) Mature *ARF17* and *5mARF17* T2 flowers with *5mARF17* petal and stamen defects increasing in severity from left to right.

5mARF17 lines with similar rosette leaf defects flowered on day 24.4 ± 1.1 ($n = 34$), 25.2 ± 1.6 ($n = 35$), 25.1 ± 1.4 ($n = 30$), 24.7 ± 1.1 ($n = 29$), and 24.3 ± 0.7 ($n = 30$), whereas nontransformed plants flowered on day 27.4 ± 1.7 ($n = 44$), and four independent *ARF17* control lines flowered on day 27.1 ± 1.6 ($n = 24$), 27.4 ± 1.2 ($n = 24$), 27.7 ± 1.4 ($n = 20$), and 27.0 ± 1.5 ($n = 20$). Despite extensive efforts, we were unable to recover a homozygous *5mARF17* plant with rosette leaf defects that was fertile.

To observe the effects of disrupting both transcriptional and miR160 regulation of *ARF17*, we transformed wild-type plants with the *5mARF17* construct under the control of the CaMV 35S promoter (*35S*:*5mARF17*). Like the *5mARF17* primary transformants, nine out of 19 *35S*:*5mARF17* primary transformants displayed embryonic (data not shown), rosette leaf (Figure 3J), and floral defects (Figures 4K and 4L). Although many of the phenotypes were qualitatively similar to those of *5mARF17* plants, the severity of leaf curling (Figure 3J) and floral organ defects (Figures 4K and 4L) and the frequency of premature death was greater in *35S*:*5mARF17* plants than *5mARF17* plants; two *35S*:*5mARF17* plants died as seedlings, four plants never transitioned to flowering but died after producing 8 to 10 upwardly curled and serrated rosette leaves, and three plants produced flowers with stamen and petal defects accompanied by reduced fertility or sterility.

5mARF17 and *35S*:*5mARF17* Plants Overaccumulate *ARF17* mRNA

RNA gel blot analysis revealed that 12- and 16-d-old *5mARF17* seedlings displaying cotyledon phenotypes (Figures 5A and 5C),

(C) to **(E)** Scanning electron micrographs of an *ARF17* T2 mature flower **(C)** and *5mARF17* T2 mature flowers with moderate floral organ defects and reduced fertility (**[D]** and **[E]**). Petal (P) length and width was reduced in *5mARF17* flowers.

(F) to **(H)** Scanning electron micrographs of *ARF17* T2 **(F)** and *5mARF17* T2 **(G)** reproductive structures. Arrowheads point to the stamen. **(H)** is a magnified view of *5mARF17* stamen. Note the reduced filament length, abnormal stamen orientation, and reduced anther size in *5mARF17* flowers. The *5mARF17* flowers in **(G)** and **(H)** were from infertile plants.

(I) Wild-type Col-0 plant floral phyllotaxy along the primary stem.

(J) *5mARF17* floral phyllotaxy along the primary and lateral stems. *5mARF17* plants have reduced fertility, illustrated by the failure to produce filled seedpods. The inset shows a magnified view of altered *5mARF17* floral phyllotaxy.

(K) Mature wild-type Col-0 flower (left) and Col-0 flower with sepals and petals removed to expose reproductive organs (right).

(L) Mature *35S*:*5mARF17* flower (left) and *35S*:*5mARF17* flower with sepals and petals removed to expose reproductive organs (right).

(M) Average hypocotyl length, primary root length, and lateral root number (expressed as a fraction of the primary root length) of 7-d-old untransformed control seedlings (C; black bars) and 7-d-old progeny of two *ARF17* T3 homozygous lines (gray bars) and two *5mARF17* T3 heterozygous lines (white bars). The *5mARF17* progeny with wild-type phenotypes (−) lacked the transgene; those with mild (+) or severe (++) phenotypes scored positive for the *5mARF17* transgene. The number of plants analyzed is indicated above each bar, and error bars represent standard deviations.

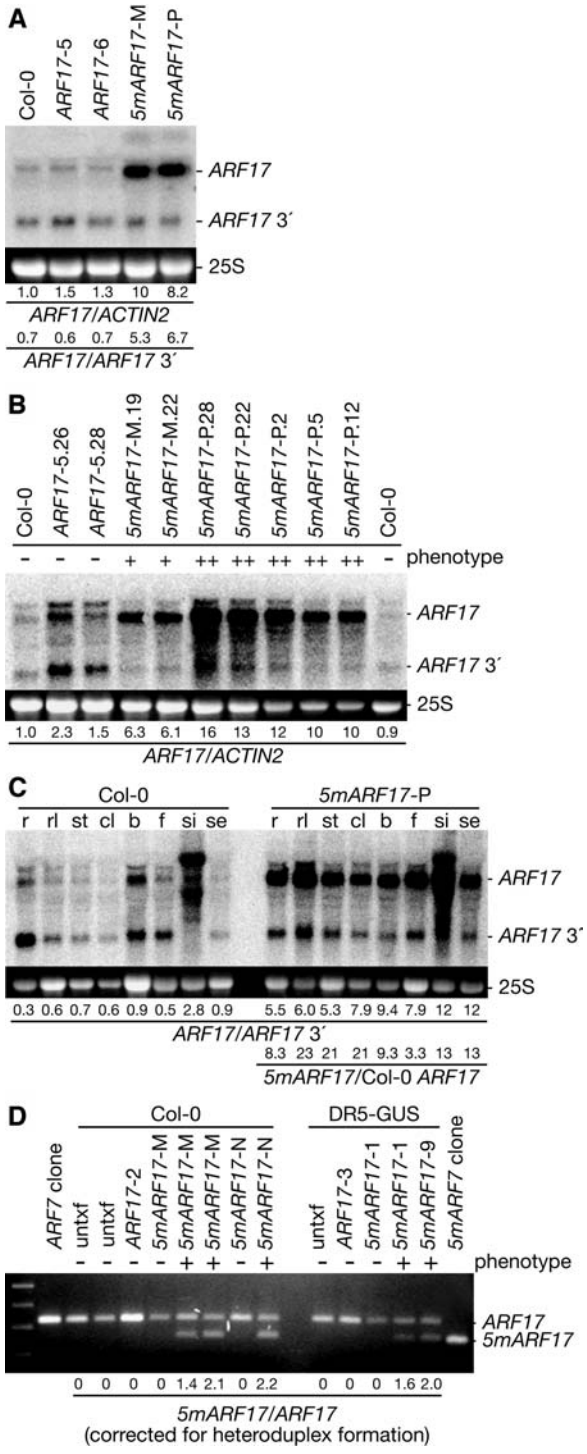

Figure 5. Phenotypic *5mARF17* Plants Accumulate Increased *ARF17* mRNA.

(A) RNA gel blot analysis of 7 μg total RNA prepared from 16-d-old T2 seedlings with a 3′ *ARF17* probe. The positions of full-length *ARF17* mRNA and *ARF17* 3′ cleavage product are noted on the right. The 25S rRNA is shown as a loading control. The blot was rehybridized with an *ACTIN2* probe, and normalized values of *ARF17* full-length mRNA to *ACTIN2* mRNA (with Col-0 levels set at 1.0) and ratios of *ARF17* full-length mRNA to 3′ cleavage product are indicated.

(B) RNA gel blot analysis of 10 μg total RNA prepared from rosette leaves of 32-d-old T2 plants with a 3′ *ARF17* probe. The absence (−) or presence of a mild (+) or severe (++) rosette leaf phenotype is indicated. The positions of full-length *ARF17* mRNA and *ARF17* 3′ cleavage products are noted at the right. Normalization was as in **(A)**.

(C) RNA gel blot analysis of 5 μg total RNA prepared from Col-0 and *5mARF17* root (r), rosette leaf (rl), stem (st), cauline leaf (cl), buds and inflorescence meristems (b), flower (f), silique and embryonic tissues (si), and 12-d-old seedling (se) tissues with a 3′ *ARF17* probe. The positions of full-length *ARF17* mRNA and *ARF17* 3′ cleavage product are noted at the right. Two uncharacterized ARF17-hybridizing RNAs, one longer and one shorter than the full-length ARF17 transcript, accumulated in siliques of Col-0 and *5mARF17* plants. Ratios of *ARF17* full-length mRNA to 3′ cleavage product are indicated, along with the relative levels of *ARF17* mRNA in *5mARF17* plants compared with wild-type Col-0 plants in each tissue (*5mARF17*/Col-0 *ARF17*).

(D) Expression of *5mARF17* mRNA in untransformed (untxf) and T2 transgenic plants that were individual progeny of the indicated primary transformant. Rosette leaf RNA was reverse transcribed, and the resulting cDNA was PCR-amplified to completion, then digested with *Apa*LI, which cuts the *5mARF17* amplicon but not the *ARF17* amplicon or heteroduplex molecules resulting from annealing *ARF17* and *5mARF17* strands. Agarose gel separation and ethidium bromide staining revealed the full-length PCR product (330 bp) and an *Apa*LI digestion fragment (250 bp). Each lane is an analysis of an individual plant, and the presence (+) or absence (−) of a rosette leaf phenotype in that plant is indicated. DNA gel blot analysis (data not shown) was used to quantitate the 330- and 250-bp DNAs, and the amount of *5mARF17* relative to *ARF17* after correcting for heteroduplex formation is shown below each lane.

as well as roots, rosette, and cauline leaves, stems, inflorescence meristems and buds, flowers, and siliques of older *5mARF17* plants with aberrant phenotypes (Figure 5C), all accumulated more *ARF17* mRNA than control plants. Moreover, *35S*:*5mARF17* transformants with aberrant phenotypes accumulated more full-length *ARF17* mRNA than *35S*:*ARF17* or untransformed wild-type Col-0 plants (Figure 1C).

The increased *ARF17* mRNA levels in *5mARF17* and *35S*:*5mARF17* plants correlated with the severity of the rosette leaf phenotype (Figures 1C and 5B). The increase was not accompanied by a similar increase in 3′ cleavage product accumulation (Figures 1 and 5), suggesting that the excess *ARF17* mRNA did not derive from the endogenous *ARF17* gene but instead derived from the *5mARF17* or *35S*:*5mARF17* transgene, which both produce mRNA refractory to miR160-directed cleavage (Figure 2B). Indeed, the fraction of *ARF17* RT-PCR product that corresponded to *5mARF17*, as monitored by *Apa*LI digestion, correlated with the presence of the rosette leaf phenotype (Figure 5D). miR160 levels were unchanged in control *ARF17* and *5mARF17* plants (data not shown), indicating that an additional copy of *ARF17* or *5mARF17* does not affect miR160 accumulation.

Because developmental defects consistent with those observed in *5mARF17* and *35S*:*5mARF17* plants were not observed in 101 control *ARF17* primary transformants or numerous progeny of these plants or 23 *35S*:*ARF17* primary transformants, we conclude that the developmental phenotypes and increased

ARF17 mRNA accumulation in *5mARF17* and *35S*:*5mARF17* plants resulted from disrupting miR160-directed *ARF17* regulation, rather than from expressing an extra copy of *ARF17*. Together, these results show that miR160 is crucial for the posttranscriptional regulation of *ARF17* expression and that this regulation is necessary for the proper growth and development of many Arabidopsis organs.

5mARF17 Plants Respond to Auxin Treatment

5mARF17 plants have fewer lateral roots and shorter hypocotyls than control plants (Figure 4M), traits characteristic of auxin-resistant mutants (Estelle and Somerville, 1987; Hobbie and Estelle, 1995; Monroe-Augustus et al., 2003). *5mARF17* plants also have shorter primary roots than control plants (Figure 4M), whereas auxin-resistant mutants typically have increased root length (Estelle and Somerville, 1987; Hobbie and Estelle, 1995; Monroe-Augustus et al., 2003). To determine if the response to exogenous auxin was altered in *5mARF17* plants, we measured root and hypocotyl length after exposing plants to the auxin IAA. Even though the primary root and hypocotyl lengths of *5mARF17* plants were shorter than those of control plants before IAA treatment, IAA treatment decreased primary root and hypocotyl growth in *5mARF17* plants (Figures 6A and 6B), indicating that *5mARF17* plants were not dramatically impaired in these responses to exogenous IAA.

IAA Treatment Does Not Appreciably Alter miR160, miR164, and miR167 Accumulation in Seedlings

In addition to miR160 and miR167, which regulate *ARF* genes (Figure 1; Rhoades et al., 2002; Kasschau et al., 2003), miR164 regulates NAC-domain genes (Laufs et al., 2004; Mallory et al., 2004a), some of which are also implicated in auxin signaling (Xie et al., 2000; Aida et al., 2002; Furutani et al., 2004). To determine whether levels of miRNAs implicated in auxin signaling are affected by exogenous IAA, we analyzed miR160, miR164, and miR167 accumulation in wild-type seedlings after IAA treatment. Although IAA treatment dramatically increased *IAA1* and *IAA19* early auxin-response transcript levels, miR160, miR164, and miR167 accumulation was not substantially altered at the times analyzed (Figure 6C), indicating that seedling levels of these miRNAs are not greatly influenced by IAA application. Similarly, *ARF17* mRNA and ARF17 3′ cleavage product levels appeared unaffected by IAA treatment (Figure 6C). These results do not provide evidence for a role of auxin in mediating *ARF17*, miR160, miR164, or miR167 expression in seedlings, suggesting that regulation by these three miRNAs may instead be needed to set components of the auxin-response machinery to proper levels so that tissues can respond appropriately to auxin.

miR160-Directed *ARF17* Regulation Is Necessary for Proper Expression of Certain *GH3*-Like Early Auxin Response Genes

Although no molecular connections between ARF10, ARF16, and ARF17 and auxin responses have been reported, these ARFs all have Pro-Ser-Thr–rich middle regions (see Supplemental Figure 1 online), suggesting that they may repress transcription of early auxin-response genes. To identify molecular changes in *5mARF17* plants, we monitored mRNA accumulation profiles of five *GH3*-like transcripts and three *Aux/IAA* transcripts in seedlings and rosette leaves. In 16-d-old seedlings, we found levels of *GH3.3* increased approximately fourfold in *5mARF17* seedlings compared with wild-type or control *ARF17* seedlings (Figure 7A), whereas levels of *IAA1 Aux/IAA* mRNA and other *GH3*-like mRNAs, *YDK1/GH3.2*, *GH3.5*, *DFL1/GH3.6*, and *DFL2/GH3.10*, were similar in wild-type, control *ARF17*, and *5mARF17* seedlings (Figure 7). In addition to an approximately fourfold increase in *GH3.3* mRNA levels, *YDK1/GH3.2* mRNA levels were increased in 30-d-old *5mARF17* rosette leaves (Figure 8A). By contrast, levels of *GH3.5* and *DFL1/GH3.6* mRNAs were decreased to undetectable levels in rosette leaves of 30-d-old *5mARF17* plants (Figure 8B), whereas levels of *DFL2/GH3.10*, *IAA1*, *IAA17*, and *IAA19* mRNAs were similar in rosette leaves of 30-d-old wild-type, control *ARF17*, and *5mARF17* plants (Figure 8A; data not shown). These results indicate that miR160-directed *ARF17* regulation is necessary for proper expression of a subset of *GH3*-like mRNAs and establish a molecular connection between ARF17 and early auxin responses.

YDK1/GH3.2, GH3.3, GH3.5, and DFL1/GH3.6 are group II GH3-like proteins that conjugate IAA to amino acids in vitro (Staswick et al., 2005) and therefore are predicted to decrease active IAA levels in the cell. To determine if responsiveness to endogenous auxin is changed in *5mARF17* plants, we expressed control *ARF17* and *5mARF17* in the widely used DR5-GUS reporter line (Guilfoyle, 1999). The DR5-GUS line expresses β-glucuronidase (GUS) under the control of a minimal CaMV 35S promoter fused to multiple copies of the TGTCTC *AuxRE*, first defined in the auxin responsive promoter of the soybean (*Glycine max*) *GH3* gene. Rosette leaves of control DR5-GUS plants transformed with control *ARF17* accumulated similar levels of *GUS* mRNA as those of the parental line (Figure 8C), and control *ARF17* DR5-GUS and DR5-GUS cotyledons and rosette leaves had a similar GUS expression pattern (data not shown). By contrast, phenotypic *5mARF17* DR5-GUS plants with increased *ARF17* mRNA levels accumulated approximately twofold more *GUS* mRNA in rosette leaves (Figure 8C). These increases correlated with more expanded GUS expression in cotyledons and rosette leaves (Figures 8D and 8E), suggesting that auxin responsiveness or perhaps auxin is more widely distributed in cotyledons and rosette leaves of *5mARF17* plants. No change in overall GUS expression was observed in roots (data not shown), suggesting that root auxin responsiveness is not greatly influenced by *5mARF17* expression. Together, these results suggest that miR160-directed regulation of *ARF17* is necessary for proper *GH3*-like gene expression and perhaps auxin distribution.

DISCUSSION

Here, we describe in vivo roles of miR160-directed *ARF17* posttranscriptional regulation. Plants expressing a miRNA-resistant version of *ARF17* (*5mARF17*) display increased *ARF17*

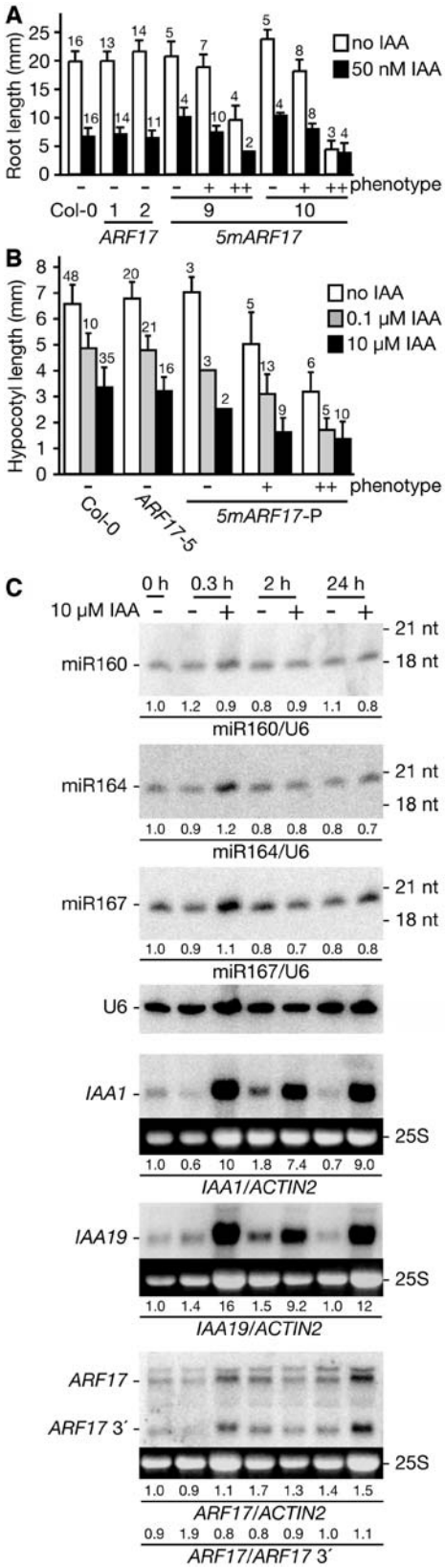

Figure 6. IAA Treatment of Wild-Type and *5mARF17* Plants.

(A) Primary root length of 8-d-old Col-0 and T2 seedlings mock treated (white bars) or treated with 50 nM IAA (black bars). *5mARF17* progeny with wild-type phenotypes (−) lacked the transgene; those with mild (+) or severe (++) phenotypes scored positive for the *5mARF17* transgene. The number of plants analyzed is indicated above each bar, and standard deviations are shown (except in cases where fewer than three plants were analyzed).

(B) Hypocotyl length of 7-d-old Col-0 and T2 seedlings mock treated (white bars) or treated with 0.1 μM IAA (gray bars) and 10 μM IAA (black bars). *5mARF17* progeny with wild-type phenotypes (−) lacked the transgene; those with mild (+) or severe (++) phenotypes scored positive for the *5mARF17* transgene. The number of plants analyzed is indicated above each bar, and standard deviations are shown (except in cases where fewer than three plants were analyzed).

(C) RNA gel blot analysis of 10 μg total RNA prepared from IAA treated (+) or untreated (−) Col-0 seedlings with DNA probes complementary to miR160, miR164, miR167, or U6 (loading control). Blots were stripped between each hybridization. The positions of ^{32}P-labeled RNA oligonucleotides are noted at the right. Also shown are RNA gel blot analyses of 10 μg of the same RNA with RNA probes complementary to *IAA1*, *IAA19*, or 3′ *ARF17*. The positions of each full-length transcript and *ARF17* 3′ cleavage product are noted at the left. The 25S rRNA is shown as a loading control. Normalized values of miRNA to U6 RNA and *IAA1*, *IAA19*, and *ARF17* full-length mRNAs to *ACTIN2* mRNA (with untreated Col-0 levels set at 1.0) and ratios of *ARF17* full-length mRNA to 3′ cleavage product are indicated.

mRNA accumulation and exhibit dramatic developmental defects. These phenotypes correlate with reduced accumulation of *GH3.5* and *DFL1/GH3.6*, two closely related mRNAs (Staswick et al., 2002), and increased accumulation of *YDK1/GH3.2* and *GH3.3*, two other closely related mRNAs (Staswick et al., 2002), as well as DR5-GUS. These results indicate that miR160-directed regulation of *ARF17* is critical for proper development, establish a molecular link between ARF17 and the auxin response pathway, and add another posttranscriptional regulatory dimension to ARF-mediated regulation.

The Developmental Abnormalities of *5mARF17* Plants Overlap with Those of Plants Impaired in miRNA Functioning

In Arabidopsis, mutations in *DCL1*, *AGO1*, *HYL1*, and *HEN1* impair the miRNA pathway and lead to developmental defects that overlap with those exhibited by *5mARF17* plants. In particular, hypomorphic *ago1* rosette leaves are serrated and *ago1*, *hyl1*, and *hen1* null mutants exhibit upwardly curled rosette leaves and a dwarfed stature. Indeed, miR160 accumulation is reduced and *ARF17* mRNA accumulation is increased in *dcl1*, *ago1*, *hyl1*, and *hen1* mutants (Kasschau et al., 2003; Vaucheret et al., 2004; Vazquez et al., 2004a), consistent with the possibility that reduced miR160-directed *ARF17* regulation contributes to the developmental abnormalities of these mutants.

Viral proteins can interfere with the miRNA pathway and affect development when expressed in plants (Mallory et al., 2002; Kasschau et al., 2003; Chapman et al., 2004; Dunoyer et al., 2004). For example, Arabidopsis plants expressing viral proteins P1/HC-Pro, p19, p15, and p21 display reduced miRNA-directed

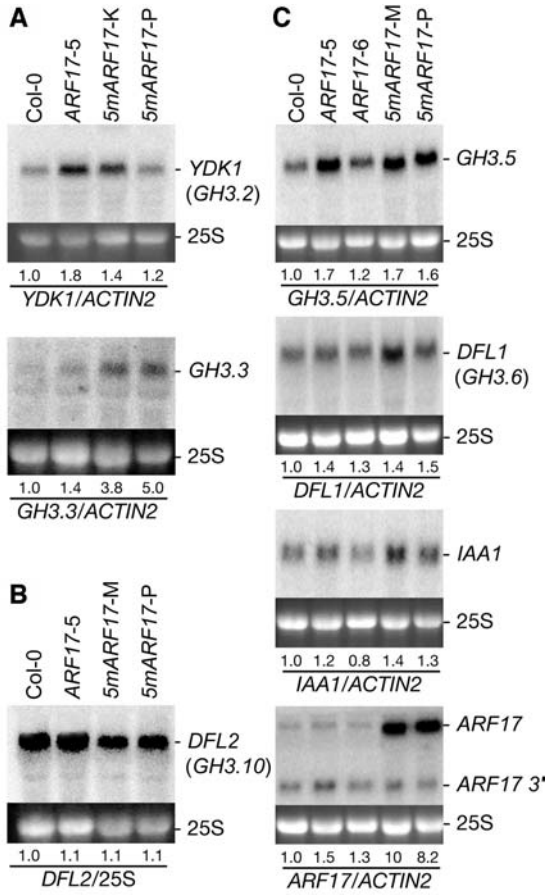

Figure 7. *GH3*-Like Expression in 16-d-Old *5mARF17* Seedlings.

(A) RNA gel blot analysis of 7 μg of total RNA from 16-d-old seedlings with RNA probes complementary to *YDK1/GH3.2* or *GH3.3.* The 25S rRNA is shown as a loading control. Blots were rehybridized with an *ACTIN2* probe, and normalized values of *GH3*-like mRNAs to *ACTIN2* mRNA are indicated, with mRNA levels in Col-0 control plants set at 1.0.
(B) Similar analysis with a probe complementary to *DFL2/GH3.10*. Normalized values of *DFL2* mRNA to 25S rRNA are indicated, with the mRNA level in Col-0 control plants set at 1.0.
(C) Similar analysis with a probe complementary to *GH3.5*, *DFL1/GH3.6*, *IAA1*, and 3′ *ARF17*. Normalizations were as in **(A)**.

mRNA cleavage and developmental abnormalities (Kasschau et al., 2003; Chapman et al., 2004; Dunoyer et al., 2004), whereas plants expressing viral proteins 2b, p38, and p25 are not impaired in miRNA-directed target mRNA cleavage and lack dramatic developmental defects (Chapman et al., 2004; Dunoyer et al., 2004). The small, serrated rosette leaf phenotypes of P1/HC-Pro, p19, p15, and p21 expressing plants (Kasschau et al., 2003; Chapman et al., 2004; Dunoyer et al., 2004) are strikingly similar to those of *5mARF17* plants (Figures 3E to 3I). In addition, P1/HC-Pro plants exhibit reduced stamen size (Kasschau et al., 2003; Chapman et al., 2004; Dunoyer et al., 2004), and p19 and p15 plants have smaller petals (Chapman et al., 2004; Dunoyer et al., 2004), also reminiscent of *5mARF17* plants (Figures 4A to 4H), suggesting that disrupted miR160-directed *ARF17* regulation can largely explain many of the developmental defects of plants expressing viral-encoded silencing suppressors.

ARF10, ARF16, and ARF17 Are Similar to Repressing ARFs

ARF proteins can either activate or repress transcription, depending on the nature of the middle domain (Ulmasov et al., 1999b). ARF5, ARF6, ARF7, ARF8, and ARF19 are activating ARFs with Gln-Leu-Ser–rich middle regions, whereas ARF1, ARF2, ARF3, ARF4, and ARF9 are repressing ARFs with Pro-Ser-Thr–rich middle regions (Ulmasov et al., 1999b; Tiwari et al., 2003). ARF10, ARF16, and ARF17 and their four rice homologs have Pro-Ser-Thr–rich middle regions (see Supplemental Figure 1 online), suggesting that they might be repressors. However, the five known repressing ARFs are more closely related to the activating ARFs than either group is to ARF10, ARF16, and ARF17 (Remington et al., 2004), so ARF10, ARF16, and ARF17 may define a specialized ARF class. *arf10* and *arf16* loss-of-function mutants do not display obvious developmental anomalies (Okushima et al., 2005). In an attempt to identify a loss-of-function *arf17* mutant, we searched the Salk Institute Genomic Analysis Laboratory collection (Alonso et al., 2003) for plants with disruptions in *ARF17*. No mutants were found with insertions in the open reading frame of *ARF17*, but one mutant, SALK_062511, had a T-DNA inserted ~210 bp upstream of the *ARF17* start codon. Plants homozygous for this insertion did not display obvious developmental defects (data not shown); however, RT-PCR revealed that these plants still accumulated *ARF17* mRNA (data not shown), indicating that this mutant was not a null allele. As has been demonstrated for other members of the ARF family (Okushima et al., 2005), functional redundancy among *ARF10*, *ARF16*, and *ARF17* may preclude informative analyses of single *arf* mutants in this class.

ARF17 Regulates *GH3*-Like Expression

There are 20 Arabidopsis *GH3* homologs, which fall into three clades. Group II GH3 proteins, including YDK1/GH3.2, GH3.3, GH3.5, and DFL1/GH3.6, conjugate IAA to amino acids in vitro (Staswick et al., 2005). Regulating IAA conjugation is important for maintaining endogenous IAA levels (Ljung et al., 2002); these GH3 proteins likely play an important role in auxin responsiveness by reducing active auxin levels and thus negatively regulating auxin signaling.

We observed decreased *GH3.5* and *DFL1/GH3.6* mRNA levels in *5mARF17* rosette leaves (Figures 8B). Because the Pro-Ser-Thr–rich middle region of ARF17 is consistent with transcriptional repression, an appealing model is that ARF17 acts directly to repress *GH3.5* and *DFL1/GH3.6* transcription, and the consequent GH3.5 and DFL1/GH3.6 reduction leads to increased IAA, which is known to stimulate the expression of *YDK1/GH3.2*, *GH3.3*, and DR5-GUS. However, because it is currently impossible to discern whether the changes in *GH3*-like transcript levels were direct or indirect consequences of disrupting miR160-directed *ARF17* regulation, there are many other possibilities. For example, ARF17 might indirectly regulate *GH3*-like and DR5-GUS expression by repressing an

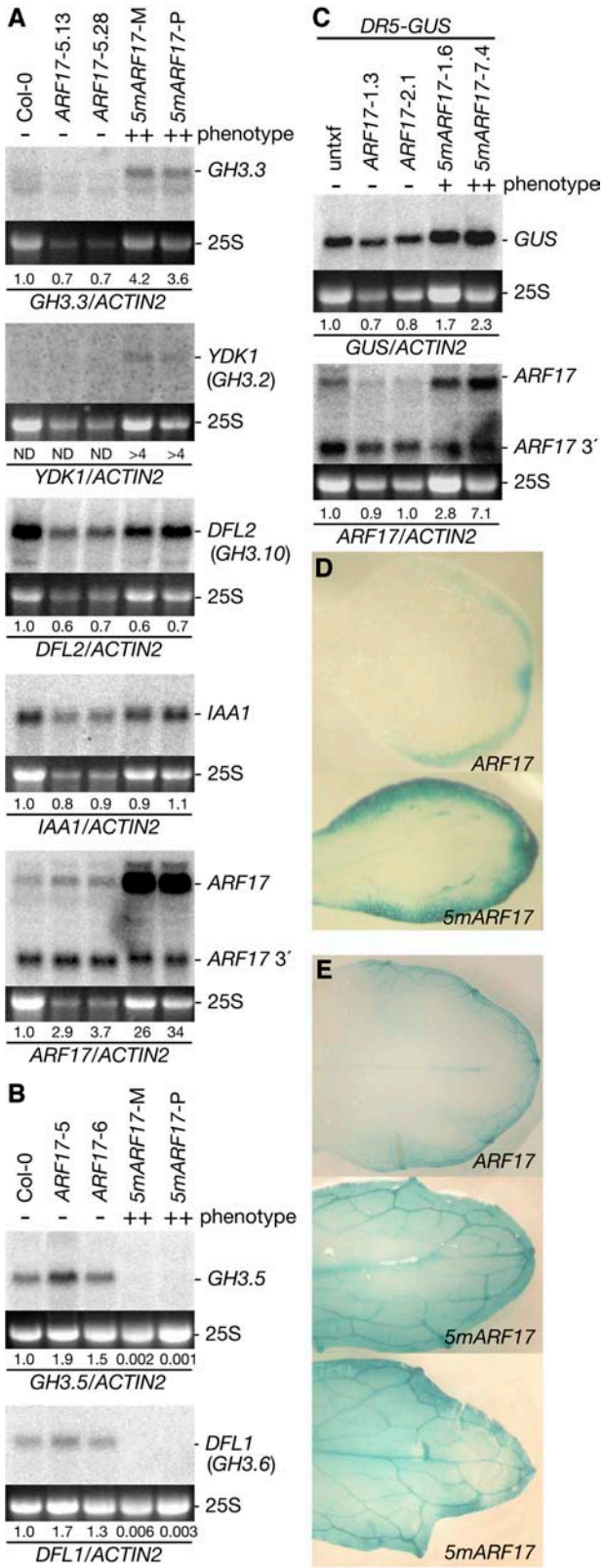

Figure 8. *GH3*-Like Gene Expression Changes in *5mARF17* Rosette Leaves.

(A) RNA gel blot analysis of 7 μg of total RNA from 30-d-old rosette leaves with RNA probes complementary to *GH3.3*, *YDK1/GH3.2*, *DFL2/GH3.10*, *IAA1*, or 3′ *ARF17*. The absence (−) or presence of a severe (++) rosette leaf phenotype is indicated. The positions of each full-length transcript and *ARF17* 3′ cleavage product are noted at the right. The 25S rRNA is shown as a loading control. Normalized values of mRNAs to *ACTIN2* mRNA are indicated, with mRNA levels in Col-0 control plants set at 1.0. Because *YDK1* transcripts were not detected (ND) in Col-0 or *ARF17* control rosette leaves, the approximately fourfold increase in YDK1 signal observed represents a minimum.

(B) Similar analysis with probes complementary to *GH3.5* or *DFL1/GH3.6*. These transcripts were not detected in *5mARF17* rosette leaves, so the fold changes observed represent a minimum.

(C) RNA gel blot analysis of 7 μg of total RNA from 30-d-old rosette leaves with RNA probes complementary to GUS or 3′ *ARF17*. The absence (−) or presence of a mild (+) or severe (++) rosette leaf phenotype is indicated. The positions of each full-length transcript and *ARF17* 3′ cleavage product are noted at the right. Normalization is as in **(A)**.

(D) Fifteen-day-old *ARF17* DR5-GUS and *5mARF17* DR5-GUS cotyledons.

(E) Twenty-eight-day-old *ARF17* DR5-GUS and *5mARF17* DR5-GUS rosette leaves with moderate (top) or more severe (bottom) leaf defects.

activator of *GH3.5* and *DFL1/GH3.6* or by repressing a repressor of *YDK1/GH3.2*, *GH3.3*, and DR5-GUS. Although the exact mechanism by which ARF17 regulates *GH3*-like gene expression is unclear, the observation that miRNA repression of *ARF17* is important for proper *GH3*-like mRNA accumulation provides an entry point for the study of early auxin-responsive gene expression.

Gain-of-Function *ydk1-D* Mutants Mimic *5mARF17* Hypocotyl and Root Phenotypes

YDK1/GH3.2 mRNA is increased in *5mARF17* rosette leaves (Figure 8A) but is not obviously changed in *5mARF17* 16-d-old seedlings (Figure 7A). Dominant *ydk1-D* mutants, which overexpress *YDK1*, have hypocotyl and root phenotypes (Takase et al., 2004) similar to *5mARF17* plants (Figure 4M). Both *5mARF17* and *ydk1-D* plants display reduced primary root length, lateral root number, hypocotyl length, and stature. *ydk1-D* plants also exhibit reduced apical dominance, which we did not observe in *5mARF17* plants. Because the hypocotyl and root phenotypes of *5mARF17* and *ydk1-D* plants are similar, it is possible that increased *YDK1* expression contributes to *5mARF17* phenotypes.

Gain-of-function *dfl1-D* plants are resistant to exogenous auxin and exhibit reduced lateral root number and hypocotyl length and a dwarf stature. Antisense *DFL1* plants have increased lateral roots (Nakazawa et al., 2001), whereas *5mARF17* plants, which show reduced *DFL1/GH3.6* mRNA accumulation in rosette leaves (Figure 8B) but not in seedlings (Figure 7C), have fewer lateral roots (Figure 4M). The expression of at least two other *GH3*-like genes, *GH3.3* and *GH3.5*, also is altered in *5mARF17* plants (Figures 7 and 8), but mutants in these genes have not been described. Because the expression of at least four *GH3*-like genes is altered in *5mARF17* plants, the

Table 1. Primer Sequences

Primer	Primer Sequence (5′–3′)
3′ ARF10 for	CAACTCTTCGGATCACCATCTCCGTC
3′ ARF10 rev	GGCCGTAATACGACTCACTATAGGCCGAGAGATCGAGTGTGCGTCC
3′ ARF16 for	GGCCGTAATACGACTCACTATAGGGGCTCCTGATGCATCCCTATAGAG
3′ ARF16 rev	GACAATGGGAACAACACCATGC
3′ ARF17 for	GAGATGATGAACTTTGGCAGTCCG
3′ ARF17 rev	GGCCGTAATACGACTCACTATAGGCCTGCGTTGCTGTTGGAATGTT
GH3.5 for	CGTGAAGTTTGCTCCAATTATCGAGC
GH3.5 rev	GGCCGTAATACGACTCACTATAGGCATGATAAAAGTCCAAACAATTCCGC
GH3.17 for	CAAGCAGAGCATGTACTGTCAGCTTC
GH3.17 rev	GGCCGTAATACGACTCACTATAGGGCCATCGAACCAGTCACAATCACC
GH3.6 for	GGCCGTAATACGACTCACTATAGGCCTTGGTGTCTTGTACTGATTGATCG
GH3.6 rev	GCGCCTCAGTTCAGCTTCATATGC
GH3.10 for	GGCCGTAATACGACTCACTATAGGGCATGTGAAACAATAGGCACCAAGG
GH3.10 rev	TTTGTCTGAAGACAAAGGGAGTGGTC
GH3.2 for	CCATCCTCTGCTCCGACTCGTCC
GH3.2 rev	GGCCGTAATACGACTCACTATAGGGCTCCAGTAACAATCACGTCGAGG
GH3.3 for	GGCCGTAATACGACTCACTATAGGGACAAGATCATTGACCGGTCACC
GH3.3 rev	GCTCTGCGATCTCCGATGATGC
IAA1 for	GGAAGTCACCAATGGGCTTAACC
IAA1 rev	GGCCGTAATACGACTCACTATAGGGCAGGAGGAGGAGCAGATTCTTCTG
IAA17 for	GGCAGTGTCGAGCTGAATCTGAGG
IAA17 rev	GGCCGTAATACGACTCACTATAGGGGCCGGAGGTTTGGCTGGATC
IAA19 for	GAGAAGGAAGGACTCGGGCTTGAG
IAA19 rev	GGCCGTAATACGACTCACTATAGGCGATGCCACGGAAACCGAAGAG
GUS for	GCGTATCGTGCTGCGTTTCGATG
GUS rev	GGCCGTAATACGACTCACTATAGGGCCTTGTCCAGTTGCAACCACC
ARF17 mut for	CGTATTCTACATTTCCTGCTGGAATGCAAGGTGCACGGCAATATGATTTTGGGTCTTTCAATCC
ARF17 mut rev	GGATTGAAAGACCCAAAATCATATTGCCGTGCACCTTGCATTCCAGCAGGAAATGTAGAATACG
ARF17 wg for	GGCCGTAATACGACTCACTATAGGCCTCTACTTATCAGGAGACCG
ARF17 wg rev	CCAGAGGACAGATTAGTGGTG
ARF10.1 RACE	CCGAGAGATCGAGTGTGCGTCC
ARF10.2 RACE	CTCCTCCGCTTCCGCCTCTTCTTCC
ARF16.1 RACE	GGCTCCTGATGCATCCCTATAGAG
ARF16.2 RACE	CCAAACCTGATGCATCATGAACTTTCTTAG
ARF17.1 RACE	CTTGGGAGCTAGAACCTGCGTTGC
ARF17.2 RACE	CCTGCGTTGCTGTTGGAATGTTTAGG
ARF17-RT for	GGATGAACCTGAGATTCTGC
ARF17-RT rev	TGGTGAATAGCTGGGGAGGATTTC
ARF17 screen	CTCTCTGTGGATCACTCTGTCTTGC
pGII far *Sac*I	GCTATGACCATGATTACGCC
ACTIN2	AACCCTCGTAGATTGGCACA

for, forward; rev, reverse; mut, mutagenesis; wg, wheat germ.

contribution of individual *GH3*-like genes to the *5mARF17* developmental defects is difficult to determine.

The expression of *GH3.5*, *DFL1*, *YDK1*, and *GH3.3* is altered in *5mARF17* rosette leaves (Figures 8A and 8B), but among the five *GH3*-like transcripts we monitored, *GH3.3* was the only transcript noticeably changed in both *5mARF17* seedlings and rosette leaves (Figures 7A and 8A). Because the increase in *ARF17* expression is consistently greater in *5mARF17* rosette leaves than in *5mARF17* seedlings (Figures 5, 7, and 8), it is possible that *ARF17* levels in seedlings are not sufficient to detectably change expression of the other *GH3*-like genes when RNA from entire seedlings is pooled for RNA gel blot analysis. Indeed, we observe expanded *DR5-GUS* expression domains not only in rosette leaves, but also in *5mARF17* cotyledons (Figures 8D and 8E), and the changes visualized by histochemical staining are obvious, whereas the changes in GUS mRNA levels are modest (approximately twofold).

miR160 and miR167 May Coordinately Modulate *GH3*-Like Expression

ARF8 appears to negatively regulate free IAA levels by controlling *GH3*-like gene expression (Tian et al., 2004). Levels of three *GH3* mRNAs, *GH3.5*, *DFL1/GH3.6*, and *GH3.17*, are reduced in *arf8* loss-of-function mutants and increased in *ARF8* overexpressing plants (Tian et al., 2004), suggesting that ARF8 activates *GH3*-like

expression. We found that miR160-directed regulation of *ARF17* is also important for proper *GH3*-like expression (Figures 7 and 8). *GH3.3* mRNA levels increase in *5mARF17* seedlings and rosette leaves, *YDK1/GH3.2* mRNA levels increase in *5mARF17* rosette leaves, and *DFL1/GH3.6* and *GH3.5* mRNA levels decrease in *5mARF17* rosette leaves (Figures 7, 8A, and 8B). Only a subset of *GH3*-like transcripts appears to be regulated by both ARF17 and ARF8; *DFL2/GH3.10* mRNA levels are unchanged in *5mARF17* rosette leaves (Figure 8A), and *GH3.3*, *DFL2/GH3.10*, and *JAR1/FIN219* mRNA levels are unchanged in *arf8* mutants and *ARF8* overexpressing plants (Tian et al., 2004).

Intriguingly, *ARF8* is regulated by miR167 (Rhoades et al., 2002; Kasschau et al., 2003), a miRNA unrelated in sequence to miR160. The miR167 complementary sites of *ARF6* and *ARF8* are in the conserved CTD (Rhoades et al., 2002; Bartel and Bartel, 2003), whereas the miR160 complementary sites in the *ARF10*, *ARF16*, and *ARF17* mRNAs (Rhoades et al., 2002) comprise the major block of conservation within the middle regions of these ARFs (see Supplemental Figure 1 online). These differences suggest independent evolutionary origins of two ARF-miRNA regulatory pairings. Although a role for miR167-directed ARF8 regulation in *GH3*-like expression remains to be examined, it is possible that miR160 and miR167 coordinately modulate *GH3*-like mRNA expression by regulating expression of repressing and activating ARF proteins encoded by *ARF17* and *ARF8*, thus contributing to the intricate interplay between auxin levels and auxin responses.

miRNAs and Auxin Signaling

In addition to *ARF* regulation by miR160 and miR167 (Rhoades et al., 2002; Kasschau et al., 2003), miR164 and miR393 also target genes implicated in auxin signaling. miR393 targets mRNAs encoding TIR1 and its three most closely related F-box proteins (Jones-Rhoades and Bartel, 2004; Sunkar and Zhu, 2004). TIR1 is the specificity component of an SCF E3 ubiquitin ligase that targets Aux/IAA proteins for ubiquitin-dependent degradation in response to auxin (Gray et al., 1999, 2001). In addition to targeting *CUC1* and *CUC2* mRNAs (Rhoades et al., 2002; Kasschau et al., 2003; Laufs et al., 2004; Mallory et al., 2004a), which establish organ boundaries in embryos and flowers (Aida et al., 1997), miR164 targets NAC1 (Rhoades et al., 2002; Mallory et al., 2004a), a putative transcription factor that promotes lateral root development downstream of TIR1 (Xie et al., 2000, 2002). Furthermore, *ARF3* and *ARF4* mRNAs over-accumulate in *zip*, *sgs3*, and *rdr6* mutants (Peragine et al., 2004); *sgs3* and *rdr6* are impaired in the accumulation of *trans*-acting short interfering RNAs, endogenous small RNAs that, like miRNAs, appear to regulate gene expression by directing mRNA cleavage (Peragine et al., 2004; Vazquez et al., 2004b). The propensity for unrelated miRNAs and possibly *trans*-acting short interfering RNAs to regulate genes involved in auxin signaling suggests that the severe developmental consequences observed when disrupting miRNA-mediated regulation of *ARF17* will be one of numerous examples in which endogenous silencing RNAs are shown to be key players modulating auxin responses during development.

METHODS

DNA Constructs, Transgenic Plants, *Agrobacterium tumefaciens*–Mediated Transient Expression, and in Vitro Cleavage Assay

The genomic sequence of *ARF17* (At1g77850), including ~1.9 and ~1.7 kb of putative 5′ and 3′ regulatory sequences, respectively, was cloned as an ~6.6-kb *Eco*RI-*Spe*I fragment into pBluescript II SK+ (Stratagene, La Jolla, CA) from the BAC F28K19. Site-directed mutagenesis using primers ARF17 mutagenesis forward and reverse (Table 1) was performed using PfuUltra polymerase followed by *Dpn*I digestion, as suggested by the manufacturer (Stratagene), to produce the *5mARF17* sequence. After mutagenesis, an ~1.9-kb *Sgr*AI-*Sex*AI fragment spanning the mutagenized *ARF17* miR160 complementary site was subcloned and used to replace the corresponding wild-type sequence of the original *ARF17* genomic clone. This 1.9-kb fragment was sequenced to ensure that only the desired silent mutations were present. The control *ARF17* and the *5mARF17* ~6.6-kb *Eco*RI-*Spe*I fragments were subcloned into binary vectors pGreenII0129 (hygromycin resistance) and pGreenII0229 (bialaphos resistance) and then electroporated into *Agrobacterium tumefaciens* strain GV3101:pMP90 (Koncz and Schell, 1986).

To generate *35S:ARF17* and *35S:5mARF17* constructs, 3.3 kb EcoR1-BamH1 fragments of each of the 6.6 kb control *ARF17* and *5mARF17* pBluescript clones described above were subcloned into pLBR19 downstream from the duplicated enhancer of CaMV 35S RNA promoter (P70) (Meyermans et al., 2000). *35S:ARF17* and *35S:5mARF17* *Kpn*I-*Eco*RI fragments were then subcloned into the binary vector pBINPLUS (kanamycin resistance) (van Engelen et al., 1995) and electroporated into Agrobacterium GV3101:pMP90.

Arabidopsis thaliana (Col-0 accession) and DR5-GUS Arabidopsis in the Col-0 accession (Guilfoyle, 1999) were transformed using the floral dip method (Clough and Bent, 1998). Collected seeds were surface sterilized and plated on Bouturage 2 medium (Duchefa Biochemie, Haarlem, The Netherlands) containing 30 μg/mL hygromycin or 50 μg/mL kanamycin for selecting Col-0 transformants or 10 μg/mL Glufosinate-ammonium PESTANAL (Sigma-Aldrich, St. Louis, MO) for selecting DR5-GUS Col-0 transformants. Seedlings were grown in long days (16 h light, 8 h dark) at 20°C for ~14 d before transfer to Metromix 200 soil (Scotts, Maysville, OH), where they were grown at 20°C in either long or short (8 h light, 16 h dark) days. For genotyping, genomic DNA from *ARF17* and *5mARF17* plants was extracted and amplified with primers ARF17 screen and pGII far *Sac*I (Table 1).

Agrobacterium infiltration of *Nicotiana benthamiana* leaves was performed as described (Llave et al., 2000). Bacteria were coinjected each at a final $OD_{600} = 0.50$, and the zones of infiltration were harvested 64 h after infiltration for total RNA isolation (Mallory et al., 2001). Expression of 35S:GUS was monitored as an infiltration control.

Arabidopsis *ARF17* transcripts containing the miR160 complementary site were generated by PCR amplification of *ARF17* or *5mARF17* genomic clones followed by in vitro transcription using T7 RNA polymerase. Primers ARF17 wheat germ forward and reverse (Table 1) were used to generate *ARF17* and *5mARF17* templates. Wheat germ lysate preparation, cap labeling, and in vitro cleavage assays were performed as described (Tang et al., 2003).

RNA Isolation, RNA Gel Blot Analysis, and 5′ RACE Analysis

Total RNA was isolated (Mallory et al., 2001) and miRNA gel blot analysis was conducted (Reinhart et al., 2002) as previously described. For mRNA gel blot analysis, RNA was separated on 1.2% agarose gels containing 0.8% formaldehyde and transferred to nylon membranes by capillary action. Blots were hybridized with α-UTP ^{32}P-labeled RNA probes at 68°C in ULTRAhyb buffer as recommended by the manufacturer (Ambion,

Austin, TX). Using the *ARF17* genomic clone (3′ ARF17 probe), pBI101 vector (GUS probe), Col-0 cDNA (At2g23170 probe), or Col-0 genomic DNA as template, ^{32}P-UTP RNA probes were generated by PCR with primers listed in Table 1 followed by T7-mediated in vitro transcription. mRNA gel blots were rehybridized with an end-labeled *ACTIN2* DNA probe. Hybridization signals were quantified using a Fuji phosphor imager (Tokyo, Japan) and normalized to *ACTIN2* or 25S rRNA for mRNA gel blot analyses or to U6 for miRNA gel blot analyses.

Poly(A)$^+$ RNA isolation, cDNA synthesis, non-gene-specific 5′ RACE amplifications and gene-specific 5′ RACE amplifications (primers listed in Table 1) were performed as described (Mallory et al., 2004a).

RT-PCR, *Apa*LI Digestion, and DNA Gel Blot Analysis

Five micrograms of total RNA prepared from rosette leaves of 30-d-old plants as described (Mallory et al., 2001) was used for $(dT)_{20}$-primed first-strand cDNA synthesis followed by RNase H digestion as recommended by the manufacturer (ThermoScript RT system; Invitrogen, Carlsbad, CA). PCR amplification using 50 ng of cDNA as template was performed to completion using ARF17-RT forward and reverse primers (Table 1). To equalize the possibility of heteroduplex formation in the *5mARF17* samples, the final PCR products were denatured and renatured. *Apa*LI digestion of the ~330-bp *5mARF17* PCR product yielded ~250- and ~80-bp fragments. To monitor *Apa*LI digestion efficiency, parallel reactions were spiked with a 2.2-kb DNA fragment containing an *Apa*LI restriction site, which produced ~1.75- and ~0.45-bp fragments after digestion. This control DNA was cleaved to completion, indicating that the undigested fragments in the *5mARF17* RT-PCR lacked the *Apa*LI site and derived from the endogenous *ARF17* gene. DNA gel blot analysis was performed as described (Mallory et al., 2001). Briefly, undigested and *Apa*LI-digested PCR amplicons were separated on a 2% agarose gel, blotted to a nylon membrane, and hybridized with ^{32}P end-labeled ARF17-RT forward primer (Table 1), which detects both undigested *ARF17* and *5mARF17* 330-bp PCR products and the 250-bp *Apa*LI digestion fragment of the *5mARF17* PCR product. Hybridization signals were quantified using a Fuji phosphor imager.

Phenotypic Analyses

Plant tissues were fixed and imaged for scanning electron microscopy as described (Mallory et al., 2004a). For histochemical staining, seedlings were submerged in a solution of 50 mM $NaPO_4$, pH 7.0, 0.5 mM $K_3Fe(CN)_6$, 0.5 mM $K_4Fe(CN)_6$, 10 mM EDTA, and 0.5 mg/mL 5-bromo-4-chloro-3-indolyl-β-D-glucuronide cyclohexylammonium salt (Gold Biotechnology, St. Louis, MO), vacuum infiltrated, and incubated 14 to 16 h at 37°C. To remove chlorophyll before photography, seedlings were rinsed repeatedly with 90% ethanol.

For seedling growth analyses, plants were grown at 20°C in long days on Bouturage 2 medium unless otherwise noted. T3 plants were grown under yellow long-pass filters (Stasinopoulos and Hangarter, 1990) to minimize IAA breakdown on horizontal plates for 7 d, after which primary root and hypocotyl lengths were measured and lateral roots were counted.

To monitor IAA-responsive transcripts, Col-0 seedlings were grown on plates for 7 d and then transferred to liquid Bouturage cultures supplemented with 0 or 10 μM IAA. Cultures were grown at 20°C with constant light and shaking (100 rpm) for the specified time, after which seedlings were collected and flash frozen with liquid nitrogen for RNA extraction.

ACKNOWLEDGMENTS

We thank M. Jones-Rhoades, G. Tang, and P. Zamore for wheat germ extracts, P. Mullineaux and R. Hellens (John Innes Centre and the Biotechnology and Biological Science Research Council, Norwich, UK) for the pGreenII0129 and pGreenII0229 binary vectors, T. Guilfoyle for DR5-GUS transgenic seeds, H. Vaucheret, M. Jones-Rhoades, and D. Dugas for critical comments on the manuscript, the W.M. Keck Foundation Biological Imaging Facility (Whitehead Institute, Cambridge, MA) for scanning electron microscope use, and T. DiCesare for graphics assistance with the cover image. The Arabidopsis Biological Resource Center at The Ohio State University (Columbus, OH) supplied the F28K19 clone and SALK 062511 seeds. This research was supported by the National Institutes of Health (F32-GM071200, A.C.M.; R24-GM069512, B.B. and D.P.B.), the G. Harold and Leila Y. Mathers Charitable Foundation (B.B.), and the Robert A. Welch Foundation (C-1309, B.B.).

Received February 9, 2005; accepted March 20, 2005.

REFERENCES

Abel, S., and Theologis, A. (1996). Early genes and auxin action. Plant Physiol. **111,** 9–17.

Achard, P., Herr, A., Baulcombe, D.C., and Harberd, N.P. (2004). Modulation of floral development by a gibberellin-regulated microRNA. Development **131,** 3357–3365.

Aida, M., Ishida, T., Fukaki, H., Fujisawa, H., and Tasaka, M. (1997). Genes involved in organ separation in Arabidopsis: An analysis of the *cup-shaped cotyledon* mutant. Plant Cell **9,** 841–857.

Aida, M., Vernoux, T., Furutani, M., Traas, J., and Tasaka, M. (2002). Roles of *PIN-FORMED1* and *MONOPTEROS* in pattern formation of the apical region of the *Arabidopsis* embryo. Development **129,** 3965–3974.

Alonso, J.M., et al. (2003). Genome-wide insertional mutagenesis of *Arabidopsis thaliana*. Science **301,** 653–657.

Ambros, V. (2004). The functions of animal microRNAs. Nature **431,** 350–355.

Aukerman, M.J., and Sakai, H. (2003). Regulation of flowering time and floral organ identity by a microRNA and its *APETALA2*-like target genes. Plant Cell **15,** 2730–2741.

Axtell, M.J., and Bartel, D.P. (2005). Antiquity of microRNAs and their targets in land plants. Plant Cell **17,** in press.

Bartel, B., and Bartel, D.P. (2003). MicroRNAs: At the root of plant development? Plant Physiol. **132,** 709–717.

Bartel, D.P. (2004). MicroRNAs: Genomics, biogenesis, mechanism, and function. Cell **116,** 281–297.

Boutet, S., Vazquez, F., Liu, J., Béclin, C., Fagard, M., Gratias, A., Morel, J.B., Crété, P., Chen, X., and Vaucheret, H. (2003). *Arabidopsis HEN1*: A genetic link between endogenous miRNA controlling development and siRNA controlling transgene silencing and virus resistance. Curr. Biol. **13,** 843–848.

Carrington, J.C., and Ambros, V. (2003). Role of microRNAs in plant and animal development. Science **301,** 336–338.

Cary, A.J., Che, P., and Howell, S.H. (2002). Developmental events and shoot apical meristem gene expression patterns during shoot development in *Arabidopsis thaliana*. Plant J. **32,** 867–877.

Chapman, E.J., Prokhnevsky, A.I., Gopinath, K., Dolja, V.V., and Carrington, J.C. (2004). Viral RNA silencing suppressors inhibit the microRNA pathway at an intermediate step. Genes Dev. **18,** 1179–1186.

Chen, J., Li, W.X., Xie, D., Peng, J.R., and Ding, S.W. (2004). Viral virulence protein suppresses RNA silencing-mediated defense but upregulates the role of microRNA in host gene expression. Plant Cell **16,** 1302–1313.

Chen, X. (2004). A microRNA as a translational repressor of *APETALA2* in *Arabidopsis* flower development. Science **303,** 2022–2025.

Clough, S.J., and Bent, A.F. (1998). Floral dip: A simplified method

for *Agrobacterium*-mediated transformation of *Arabidopsis thaliana*. Plant J. **16,** 735–743.

Dharmasiri, S., and Estelle, M. (2002). The role of regulated protein degradation in auxin response. Plant Mol. Biol. **49,** 401–409.

Dugas, D.V., and Bartel, B. (2004). MicroRNA regulation of gene expression in plants. Curr. Opin. Plant Biol. **7,** 512–520.

Dunoyer, P., Lecellier, C.H., Parizotto, E.A., Himber, C., and Voinnet, O. (2004). Probing the microRNA and small interfering RNA pathways with virus-encoded suppressors of RNA silencing. Plant Cell **16,** 1235–1250.

Emery, J.F., Floyd, S.K., Alvarez, J., Eshed, Y., Hawker, N.P., Izhaki, A., Baum, S.F., and Bowman, J.L. (2003). Radial patterning of *Arabidopsis* shoots by class III *HD-ZIP* and *KANADI* genes. Curr. Biol. **13,** 1768–1774.

Estelle, M., and Somerville, C. (1987). Auxin-resistant mutants of *Arabidopsis thaliana* with an altered morphology. Mol. Gen. Genet. **206,** 200–206.

Floyd, S.K., and Bowman, J.L. (2004). Gene regulation: Ancient microRNA target sequences in plants. Nature **428,** 485–486.

Friml, J. (2003). Auxin transport: Shaping the plant. Curr. Opin. Plant Biol. **6,** 7–12.

Furutani, M., Vernoux, T., Traas, J., Kato, T., Tasaka, M., and Aida, M. (2004). *PIN-FORMED1* and *PINOID* regulate boundary formation and cotyledon development in *Arabidopsis* embryogenesis. Development **131,** 5021–5030.

Gray, W.M., del Pozo, J.C., Walker, L., Hobbie, L., Risseeuw, E., Banks, T., Crosby, W.L., Yang, M., Ma, H., and Estelle, M. (1999). Identification of an SCF ubiquitin-ligase complex required for auxin response in *Arabidopsis thaliana*. Genes Dev. **13,** 1678–1691.

Gray, W.M., Kepinski, S., Rouse, D., Leyser, O., and Estelle, M. (2001). Auxin regulates SCF(TIR1)-dependent degradation of AUX/IAA proteins. Nature **414,** 271–276.

Guilfoyle, T.J. (1999). Auxin-regulated genes and promoters. In Biochemistry and Molecular Biology of Plant Hormones, P.J.J. Hooykaas, M.A. Hall, and K.R. Libbenga, eds (Amsterdam: Elsevier), pp. 423–459.

Guilfoyle, T.J., and Hagen, G. (2001). Auxin response factors. J. Plant Growth Regul. **10,** 281–291.

Guilfoyle, T.J., Ulmasov, T., and Hagen, G. (1998). The ARF family of transcription factors and their role in plant hormone-responsive transcription. Cell. Mol. Life Sci. **54,** 619–627.

Hagen, G., and Guilfoyle, T. (2002). Auxin-responsive gene expression: Genes, promoters and regulatory factors. Plant Mol. Biol. **49,** 373–385.

Han, M.H., Goud, S., Song, L., and Fedoroff, N. (2004). The *Arabidopsis* double-stranded RNA-binding protein HYL1 plays a role in microRNA-mediated gene regulation. Proc. Natl. Acad. Sci. USA **101,** 1093–1098.

Hobbie, L., and Estelle, M. (1995). The *axr4* auxin-resistant mutants of *Arabidopsis thaliana* define a gene important for root gravitropism and lateral root initiation. Plant J. **7,** 211–220.

Hutvágner, G., and Zamore, P.D. (2002). A microRNA in a multiple-turnover RNAi enzyme complex. Science **297,** 2056–2060.

Jones-Rhoades, M.W., and Bartel, D.P. (2004). Computational identification of plant miRNAs and their targets, including a stress-induced miRNA. Mol. Cell **14,** 787–799.

Juarez, M.T., Kui, J.S., Thomas, J., Heller, B.A., and Timmermans, M.C. (2004). microRNA-mediated repression of *rolled leaf1* specifies maize leaf polarity. Nature **428,** 84–88.

Jürgens, G. (2003). Growing up green: Cellular basis of plant development. Mech. Dev. **120,** 1395–1406.

Kasschau, K.D., Xie, Z., Allen, E., Llave, C., Chapman, E.J., Krizan, K.A., and Carrington, J.C. (2003). P1/HC-Pro, a viral suppressor of RNA silencing, interferes with *Arabidopsis* development and miRNA function. Dev. Cell **4,** 205–217.

Kepinski, S., and Leyser, O. (2002). Ubiquitination and auxin signaling: A degrading story. Plant Cell **14** (suppl.), S81–S95.

Kim, J., Harter, K., and Theologis, A. (1997). Protein-protein interactions among the Aux/IAA proteins. Proc. Natl. Acad. Sci. USA **94,** 11786–11791.

Koncz, C., and Schell, J. (1986). The promoter of the T_L-DNA gene 5 controls the tissue-specific expression of chimaeric genes carried by a novel type of *Agrobacterium* binary vector. Mol. Gen. Genet. **204,** 383–396.

Laufs, P., Peaucelle, A., Morin, H., and Traas, J. (2004). MicroRNA regulation of the *CUC* genes is required for boundary size control in *Arabidopsis* meristems. Development **131,** 4311–4322.

Lee, R.C., Feinbaum, R.L., and Ambros, V. (1993). The *C. elegans* heterochronic gene *lin-4* encodes small RNAs with antisense complementarity to *lin-14*. Cell **75,** 843–854.

Lewis, B.P., Burge, C.B., and Bartel, D.P. (2005). Conserved seed pairing, often flanked by adenosines, indicates that thousands of human genes are microRNA targets. Cell **120,** 15–20.

Lim, L.P., Lau, N.C., Garrett-Engele, P., Grimson, A., Schelter, J.M., Castle, J., Bartel, D.P., Linsley, P.S., and Johnson, J.M. (2005). Microarray analysis shows that some microRNAs downregulate large numbers of target mRNAs. Nature **433,** 769–773.

Liscum, E., and Reed, J.W. (2002). Genetics of Aux/IAA and ARF action in plant growth and development. Plant Mol. Biol. **49,** 387–400.

Ljung, K., Hull, A.K., Kowalczyk, M., Marchant, A., Celenza, J., Cohen, J.D., and Sandberg, G. (2002). Biosynthesis, conjugation, catabolism and homeostasis of indole-3-acetic acid in *Arabidopsis thaliana*. Plant Mol. Biol. **49,** 249–272.

Llave, C., Kasschau, K.D., and Carrington, J.C. (2000). Virus-encoded suppressor of posttranscriptional gene silencing targets a maintenance step in the silencing pathway. Proc. Natl. Acad. Sci. USA **97,** 13401–13406.

Llave, C., Xie, Z., Kasschau, K.D., and Carrington, J.C. (2002). Cleavage of *Scarecrow-like* mRNA targets directed by a class of *Arabidopsis* miRNA. Science **297,** 2053–2056.

Mallory, A.C., Dugas, D.V., Bartel, D.B., and Bartel, B. (2004a). MicroRNA regulation of NAC-domain targets is required for proper formation and separation of adjacent embryonic, vegetative, and floral organs. Curr. Biol. **14,** 1035–1046.

Mallory, A.C., Ely, L., Smith, T.H., Marathe, R., Anandalakshmi, R., Fagard, M., Vaucheret, H., Pruss, G., Bowman, L., and Vance, V.B. (2001). HC-Pro suppression of transgene silencing eliminates the small RNAs but not transgene methylation or the mobile signal. Plant Cell **13,** 571–583.

Mallory, A.C., Reinhart, B.J., Bartel, D.P., Vance, V.B., and Bowman, L.H. (2002). A viral suppressor of RNA silencing differentially regulates the accumulation of short interfering RNAs and micro-RNAs in tobacco. Proc. Natl. Acad. Sci. USA **99,** 15228–15233.

Mallory, A.C., Reinhart, B.J., Jones-Rhoades, M.W., Tang, G., Zamore, P.D., Barton, M.K., and Bartel, D.P. (2004b). MicroRNA control of *PHABULOSA* in leaf development: Importance of pairing to the microRNA 5′ region. EMBO J. **23,** 3356–3364.

Mallory, A.C., and Vaucheret, H. (2004). MicroRNAs: Something important between the genes. Curr. Opin. Plant Biol. **7,** 120–125.

McHale, N.A., and Koning, R.E. (2004). MicroRNA-directed cleavage of *Nicotiana sylvestris PHAVOLUTA* mRNA regulates the vascular cambium and structure of apical meristems. Plant Cell **16,** 1730–1740.

Meyermans, H., et al. (2000). Modifications in lignin and accumulation of phenolic glucosides in poplar xylem upon down-regulation of caffeoyl-Coenzyme A O-methyltransferase, an enzyme involved in lignin biosynthesis. J. Biol. Chem. **275,** 36899–36909.

Monroe-Augustus, M., Zolman, B.K., and Bartel, B. (2003). IBR5, a dual-specificity phosphatase-like protein modulating auxin and abscisic acid responsiveness in Arabidopsis. Plant Cell **15,** 2979–2991.

Nakazawa, M., Yabe, N., Ichikawa, T., Yamamoto, Y.Y., Yoshizumi, T., Hasunuma, K., and Matsui, M. (2001). *DFL1*, an auxin-responsive *GH3* gene homologue, negatively regulates shoot cell elongation and lateral root formation, and positively regulates the light response of hypocotyl length. Plant J. **25,** 213–221.

Okushima, Y., et al. (2005). Functional genomic analysis of the *AUXIN RESPONSE FACTOR* gene family members in *Arabidopsis thaliana*: Unique and overlapping functions of *ARF7* and *ARF19*. Plant Cell **17,** 444–463.

Olsen, P.H., and Ambros, V. (1999). The *lin-4* regulatory RNA controls developmental timing in *Caenorhabditis elegans* by blocking LIN-14 protein synthesis after the initiation of translation. Dev. Biol. **216,** 671–680.

Palatnik, J.F., Allen, E., Wu, X., Schommer, C., Schwab, R., Carrington, J.C., and Weigel, D. (2003). Control of leaf morphogenesis by microRNAs. Nature **425,** 257–263.

Parizotto, E.A., Dunoyer, P., Rahm, N., Himber, C., and Voinnet, O. (2004). In vivo investigation of the transcription, processing, endonucleolytic activity, and functional relevance of the spatial distribution of a plant miRNA. Genes Dev. **18,** 2237–2242.

Park, W., Li, J., Song, R., Messing, J., and Chen, X. (2002). CARPEL FACTORY, a Dicer homolog, and HEN1, a novel protein, act in microRNA metabolism in *Arabidopsis thaliana*. Curr. Biol. **12,** 1484–1495.

Peragine, A., Yoshikawa, M., Wu, G., Albrecht, H.L., and Poethig, R.S. (2004). SGS3 and SGS2/SDE1/RDR6 are required for juvenile development and the production of trans-acting siRNAs in *Arabidopsis*. Genes Dev. **18,** 2368–2379.

Reed, J.W. (2001). Roles and activities of Aux/IAA proteins in *Arabidopsis*. Trends Plant Sci. **6,** 420–425.

Reinhart, B.J., Weinstein, E.G., Rhoades, M.W., Bartel, B., and Bartel, D.P. (2002). MicroRNAs in plants. Genes Dev. **16,** 1616–1626.

Remington, D.L., Vision, T.J., Guilfoyle, T.J., and Reed, J.W. (2004). Contrasting modes of diversification in the *Aux/IAA* and *ARF* gene families. Plant Physiol. **135,** 1738–1752.

Rhoades, M., Reinhart, B., Lim, L., Burge, C., Bartel, B., and Bartel, D. (2002). Prediction of plant microRNA targets. Cell **110,** 513–520.

Rogg, L.E., and Bartel, B. (2001). Auxin signaling: Derepression through regulated proteolysis. Dev. Cell **1,** 595–604.

Rouse, D., Mackay, P., Stirnberg, P., Estelle, M., and Leyser, O. (1998). Changes in auxin response from mutations in an *AUX/IAA* gene. Science **279,** 1371–1373.

Stasinopoulos, T.C., and Hangarter, R.P. (1990). Preventing photochemistry in culture media by long-pass light filters alters growth of cultured tissues. Plant Physiol. **93,** 1365–1369.

Staswick, P.E., Serban, B., Rowe, M., Tiryaki, I., Maldonado, M.T., Maldonado, M.C., and Suza, W. (2005). Characterization of an Arabidopsis enzyme family that conjugates amino acids to indole-3-acetic acid. Plant Cell **17,** 616–627.

Staswick, P.E., Tiryaki, I., and Rowe, M.L. (2002). Jasmonate response locus *JAR1* and several related Arabidopsis genes encode enzymes of the firefly luciferase superfamily that show activity on jasmonic, salicylic, and indole-3-acetic acids in an assay for adenylation. Plant Cell **14,** 1405–1415.

Sunkar, R., and Zhu, J.K. (2004). Novel and stress-regulated microRNAs and other small RNAs from Arabidopsis. Plant Cell **16,** 2001–2019.

Swarup, R., Parry, G., Graham, N., Allen, T., and Bennett, M. (2002). Auxin cross-talk: Integration of signalling pathways to control plant development. Plant Mol. Biol. **49,** 411–426.

Takase, T., Nakazawa, M., Ishikawa, A., Kawashima, M., Ichikawa, T., Takahashi, N., Shimada, H., Manabe, K., and Matsui, M. (2004). *ydk1-D*, an auxin-responsive *GH3* mutant that is involved in hypocotyl and root elongation. Plant J. **37,** 471–483.

Tang, G., Reinhart, B.J., Bartel, D.P., and Zamore, P.D. (2003). A biochemical framework for RNA silencing in plants. Genes Dev. **17,** 49–63.

Tian, C.E., Muto, H., Higuchi, K., Matamura, T., Tatematsu, K., Koshiba, T., and Yamamoto, K.T. (2004). Disruption and overexpression of *auxin response factor 8* gene of *Arabidopsis* affect hypocotyl elongation and root growth habit, indicating its possible involvement in auxin homeostasis in light condition. Plant J. **40,** 333–343.

Tiwari, S.B., Hagen, G., and Guilfoyle, T. (2003). The roles of auxin response factor domains in auxin-responsive transcription. Plant Cell **15,** 533–543.

Tiwari, S.B., Hagen, G., and Guilfoyle, T.J. (2004). Aux/IAA proteins contain a potent transcriptional repression domain. Plant Cell **16,** 533–543.

Ulmasov, T., Hagen, G., and Guilfoyle, T.J. (1997). ARF1, a transcription factor that binds to auxin response elements. Science **276,** 1865–1868.

Ulmasov, T., Hagen, G., and Guilfoyle, T.J. (1999a). Dimerization and DNA binding of auxin response factors. Plant J. **19,** 309–319.

Ulmasov, T., Hagen, G., and Guilfoyle, T.J. (1999b). Activation and repression of transcription by auxin-response factors. Proc. Natl. Acad. Sci. USA **96,** 5844–5849.

van Engelen, F.A., Molthoff, J.W., Conner, A.J., Nap, J.P., Pereira, A., and Stiekema, W.J. (1995). pBINPLUS: An improved plant transformation vector based on pBIN19. Transgenic Res. **4,** 288–290.

Vaucheret, H., Vazquez, F., Crété, P., and Bartel, D.P. (2004). The action of *ARGONAUTE1* in the miRNA pathway and its regulation by the miRNA pathway are crucial for plant development. Genes Dev. **18,** 1187–1197.

Vazquez, F., Gasciolli, V., Crété, P., and Vaucheret, H. (2004a). The nuclear dsRNA binding protein HYL1 is required for microRNA accumulation and plant development, but not posttranscriptional transgene silencing. Curr. Biol. **14,** 346–351.

Vazquez, F., Vaucheret, H., Rajagopalan, R., Lepers, C., Gasciolli, V., Mallory, A.C., Hilbert, J.L., Bartel, D.P., and Crete, P. (2004b). Endogenous trans-acting siRNAs regulate the accumulation of *Arabidopsis* mRNAs. Mol. Cell **16,** 69–79.

Wang, J.F., Zhou, H., Chen, Y.Q., Luo, Q.J., and Qu, L.H. (2004a). Identification of 20 microRNAs from *Oryza sativa*. Nucleic Acids Res. **32,** 1688–1695.

Wang, X.J., Reyes, J.L., Chua, N.H., and Gaasterland, T. (2004b). Prediction and identification of *Arabidopsis thaliana* microRNAs and their mRNA targets. Genome Biol. **5,** R65.

Wightman, B., Ha, I., and Ruvkun, G. (1993). Posttranscriptional regulation of the heterochronic gene *lin-14* by *lin-4* mediates temporal pattern formation in *C. elegans*. Cell **75,** 855–862.

Xie, Q., Frugis, G., Colgan, D., and Chua, N.-H. (2000). *Arabidopsis* NAC1 transduces auxin signal downstream of TIR1 to promote lateral root development. Genes Dev. **14,** 3024–3036.

Xie, Q., Guo, H.-S., Dallman, G., Fang, S., Weissman, A.M., and Chua, N.-H. (2002). SINAT5 promotes ubiquitin-related degradation of NAC1 to attenuate auxin signals. Nature **419,** 167–170.

Xie, Z., Kasschau, K.D., and Carrington, J.C. (2003). Negative feedback regulation of *Dicer-Like1* in *Arabidopsis* by microRNA-guided mRNA. Curr. Biol. **13,** 784–789.

Yekta, S., Shih, I.H., and Bartel, D.P. (2004). MicroRNA-directed cleavage of *HOXB8* mRNA. Science **304,** 594–596.

Zhong, R., and Ye, Z.H. (2004). *amphivasal vascular bundle 1*, a gain-of-function mutation of the *IFL1/REV* gene, is associated with alterations in the polarity of leaves, stems and carpels. Plant Cell Physiol. **45,** 369–385.